universität wien

MASTERARBEIT / MASTER'S THESIS

Titel der Masterarbeit / Title of the Master's Thesis

„Salinity driven speciation through fine-scale morphological adaptations in the dinoflagellate species flock *Peridinium aciculiferum/Scrippsiella hangoei*"

verfasst von / submitted by

Alina Wiemers, BSc.

angestrebter akademischer Grad / in partial fulfilment of the requirements for the degree of

Master of Science (MSc)

Wien, 2016 / Vienna, 2016

Studienkennzahl lt. Studienblatt / degree programme code as it appears on the student record sheet:	A 066 833
Studienrichtung lt. Studienblatt / degree programme as it appears on the student record sheet:	Masterstudium Ecology and Ecosystems
Betreut von / Supervisor:	Prof. Karin Rengefors, PhD

“It always seems impossible until it's done.”

- Nelson Mandela

Table of contents

List of Figures

List of Tables

Introduction

Dinoflagellates are ubiquitous unicellular eukaryotes with important ecological roles in marine and freshwater ecosystems (Logares et al., 2008) and belong to the superphylum Alveolata (Lewis et al., 2013). They have a high diversity of life strategies, with symbionts, parasites, photosynthesizers, heterotrophs and mixotrophs (Hackett et al., 2004). Dinoflagellates display tremendous morphological diversity and are important primary producers in marine environments (Coelho et al., 2013). A number of dinoflagellate species are known to produce potent neurotoxins, which are often associated with the phenomena commonly called ‘‘red tides’’ (Hackett et al., 2004). Also, dinoflagellates have become more and more dominant relative to diatoms, in spring blooms in some parts of the Baltic Sea since the last decades (Klais et al., 2011; Wasmund, 2003; Wasmund et al., 1998). Suikkanen et al. (2011) concluded that spring bloom forming dinoflagellates may outcompete diatoms via allelopathic effects.

In the northern Baltic Sea *Scrippsiella hangoei* (Schiller) forms under ice blooms and is one of the most abundant species during the winter-spring season (Kremp, 2000; Larsen et al., 1995). Rengefors and Legrand (2007) found that *Peridinium aciculiferum* showed a highly variable allelopathic activity. This species occurs in large numbers in winter phytoplankton communities and forms blooms under ice in some Swedish lakes (Rengefors and Anderson, 1998; Rengefors and Legrand, 2007, 2001). Along the coast of Finland “red-tides” of cold-water dinoflagellates have become common events since the 1980s (Kremp et al., 2005; Kuosa, 1986; Larsen et al., 1995; Lignell et al., 1993). Therefore it is important to know what drives marine-freshwater transitions of potentially toxic dinoflagellate species.

Marine and fresh waters are two environments which differ in their general physicochemical characteristics. The differences in osmotic pressure and ionic concentrations between marine and fresh waters represent a strong barrier that cannot be crossed by most species. Phylogenetic analyses of dinoflagellates showed that marine-freshwater transitions are rare and marine and freshwater species are usually not closely related. (Logares et al., 2007b) These infrequency of transitions (gene flow) between marine and fresh waters, as well as the different physicochemical and ecological conditions in each environment, has likely promoted the evolution of locally adapted lineages (Logares et al., 2009).

The dinoflagellate species flock composed of the marine-brackish species *Scrippsiella hangoei* and *Scrippsiella* aff. *hangoei*, the freshwater species *Peridinium aciculiferum*, *Peridinium baicalense*, *Peridinium* euryceps and *Scrippsiella hangoei* from Lake Baikal revealed to be very closely related (Logares et al., 2008, 2007a, 2007b; Rengefors et al., 2008; Annenkova et al., 2015). They have identical SSU rDNA fragments and distinct but very small differences in the DNA markers LSU rDNA, ITS2 and COB gene, which are used to delineate dinoflagellate species (Annenkova et al., 2015). *S.* aff. *hangoei* differs from *S. hangoei* in about 1% of the basepairs in the rRNA sequences

(Rengefors et al., 2008). *P. aciculiferum* has probably colonized freshwaters very recently, due to the fact that it is very closely related to the marine-brackish *S. hangoei*, and both morphospecies cluster with marine-brackish species (Logares et al., 2007a, 2007b).

Annenkova et al. (2015) suggest that this species flock could be a case of recent rapid adaptive radiation in response to changes in the environment, due to the small but species–specific sequence differences and the co-occurrence of some species. This species flock with small genetic differences is characterized by relatively large distinct morphological differences and differences in salinity tolerance (Annenkova et al., 2015). Studies from another cold-water dinoflagellates indicate local adaptation favoured by salinity differences (Rengefors et al., 2015). In heterogeneous environments, provided that there are no costs of phenotypic plasticity, phenotypic rather than genetic differentiation would evolve (Kawecki and Ebert, 2004). This would mean that multiple phenotypes can be produced from a single genotype when exposed to different environmental conditions (Rengefors et al., 2015).

Four morphospecies can be distinguished, one single saline morphospecies *S. hangoei* including *S.* aff. *hangoei*, and three freshwater morphospecies (*P. aciculiferum*, *P. euryceps*, *P. baicalense*). All morphospecies occur in freshwater environments only except *S. hangoei*, which has a wide salinity tolerance (0-30) and is also found in marine-brackish environments in the Baltic Sea and polar oceans. Logares et al., (2008) suggested differences in water salinity as the main driver of speciation between *P. aciculiferum* and *S. hangoei*. However, this does not explain the presence of *S. hangoei* in freshwater Lake Baikal and its absence in Lake Erken (Annenkova et al., 2015). The *P. aciculiferum* morphospecies has a sub-spherical morphology with the presence of spines, whereas the *S. hangoei* morphospecies is egg-shaped with the absence of spines (Logares et al., 2007a). The cells of *P. aciculiferum* have 3–4 small antapical spines and cells of *P. euryceps* two pronounced antapical spines (Annenkova et al., 2015). The *P. baicalense* morphospecies is the biggest and most elongated and cells have two prominent horns on each of the antapical plates and one less pronounced lateral horn (Annenkova et al., 2015).

Salinity differences of aquatic environments also affect the water density. Seawater density at 4°C is approximately 1.02822 g ml^{-1}, while freshwater has a density of 1.0000 g ml^{-1} (Wetzel, 2001). Still dinoflagellates are denser than both saline and fresh waters (e.g. 1.082-1.094 g ml^{-1}; Kamykowski et al., 1992) and therefore need to swim or use other adaptations to stay buoyant. Dinoflagellates have an increased sinking velocity with size, but a decreased sinking velocity with a larger surface area to volume ratio (Kamykowski et al., 1992). So species with a high swim to sink ratio will ascend easier than those with a low ratio (Kamykowski et al., 1992).

Saline water has a higher density then fresh water and therefore the selection pressure on cell shape and size to remain suspended in the water, should be much higher in freshwater than in seawater. Therefore we would expect differences in morphology between the two environments. Cell properties

such as spines and a flattened cell shape would increase surface area and thereby decrease sinking velocity and would be dominate in freshwater. In saline waters the spherical morphology would dominate.

Aim of the project

The aim of this project is to determine fine-scale morphological adaptations to minimize sinking in response to salinity differences, in the dinoflagellate species complex *P. aciculiferum – S. hangoei*. Salinity affects the water density and therefore may act as a driver of speciation due to strong selective pressure on morphology.

Furthermore, I wanted to investigate the absence of the dinoflagellate species *S. hangoei* in Swedish freshwater lakes even though *S. hangoei* can grow in a wide range of salinities (0-30) and occurs in both the brakish Baltic Sea and the freshwater Lake Baikal (Annenkova et al., 2015). In Lake Baikal convective currents can occur, resulting in vertical mixing of the upper water column that can extend to 30-50m depth (Richardson et al., 2000). In contrast at Lake Erken, oscillating currents can occur, generating horizontal movements (Malm et al., 1998). *S. hangoei* could depend on vertical mixing to stay at the surface layers, due to morphological constraints. In the Baltic Sea the mean irradiances measured during the winter months were 0.1, 1, 10 and 100 µmol photons m^{-2} s^{-1} in water depths of 15, 10, 5 and 1 m respectively (Kremp, 2001). Phytoplankton often experience light fluctuations between high light and low light or darkness as a result of the vertical mixing of the water column (Litchman and Klausmeier, 2001). Therefore I submitted *P. aciculiferum and S. hangoei* to competition under constant and fluctuating light conditions.

Here I present data on different morphological parameters and growth rate of *P. aciculiferum*, *S. hangoei* and *P. baicalense* originating from 8 different locations. Also the cell densities and mean percentages of *P. aciculiferum* and *S. hangoei* under competition are shown.

The following hypothesis were set up:

H1: Species in freshwater (low density) have a morphology that will lower sinking rate, while in saline water (high density) have retained a spherical shape with high sinking rate.

H2: The species adapted to vertical mixing will dominate under fluctuating light conditions, while the species adapted to non or horizontal movements will dominate under stable light conditions.

Material and Methods

Algal Cultures

For the experiments, algae cultures previously collected from 8 different locations, were set up (see pictures, Appendix, Figure 10). All salinity values are given as Practical Salinity Scale and are presented without units. For the *P. aciculiferum* morphospecies strains from Lake Erken in Sweden and from Lake Østre Anlæg ved Sølvtorvet in Copenhagen were chosen. Both locations are freshwater lakes with a salinity of 0. Lake Østre Anlæg ved Sølvtorvet in Copenhagen was sampled by Moestrup and isolated by Khandan 2014. Lake Erken is located north of Stockholm around 15 km away from the Baltic Sea at 11.1 m asl (Logares et al., 2007a). It's a moderately eutrophic lake with a mean depth of 9 m, a maximum depth of 21 m and a surface area of 23.7 km² (Pettersson, 1980). Lake Erken was disconnected from the Baltic Sea ~3000 years ago by isostatic uplift (Ekman and Fries, 1970) and is ice-covered for ~ 4 months a year from January till end of April (Pettersson, 1980).

For the *S.* aff. *hangoei* populations of the *S. hangoei* morphospecies, two lakes with different salinities located in the Vestfold Hills area, Antarctica were selected. The location is part of the ice-free coastal area of Princess Elizabeth Land and was formed ~6000 years ago by isostatic uplift (Zwartz et al., 1998). These lakes include Lake Abraxas with a salinity between 14-17 and Lake McNeil with a salinity of 6 (Rengefors et al., 2012). Both lakes are marine derived and hydrologically unconnected (Laybourn-Parry and Pearce, 2007). The lakes in the Vestfold Hills area are usually ice covered but for 1 – 2 month ice free during the summer (Rengefors et al., 2012). The *S.* aff. *hangoei* populations were sampled during the Antarctic summer 2009 (Rengefors et al., 2012) and previously identified in Rengefors et al., 2008.

Two populations of the *S. hangoei* morphospecies from the Baltic Sea were selected. The Tvärminne sampling site is located near the entrance of the Gulf of Finland with a salinity between 5 – 8 (Logares et al., 2007a). The *S. hangoei* strains from Tvärminne were isolated by A. Kremp 2009 and C. Sjöqvist 2010. The second *S. hangoei* Baltic Sea population was collected from the Gulf of Finland, HELCOM monitoring station LL7 of Helsinki and isolated by A. Kremp in 2013. The salinity from the Gulf of Finland lies between 3-7 (Omstedt and Axell, 2003). The pristine freshwater Baltic Sea was starting to rise in salinity when it was connected to the North Sea after glaciation ~8500 years ago (Logares et al., 2008).

Table 1: Description of sampling sites

Water reservoir	Location	Coordinates	Salinity (Psu)	Species	Strain	References
Lake Abraxas	Antarctica	S-68°29' E-78°17'	14-17	*S. aff. hangoei*	Abra	(Rengefors et al., 2012)
Lake McNeil	Antarctica	S-68°31' E-78°21'	6	*S. aff. hangoei*	McNeil	(Rengefors et al., 2012)
Gulf of Finland Baltic sea	Finland	N-60°00' E-24°50'	3-7	*S. hangoei*	SHLL7	(Omstedt and Axell, 2003)
Tvärminne Baltic sea	Finland	N-59°50' E- 23°15'	5-8	*S. hangoei*	SHTV	(Logares et al., 2008)
Sludyanka Lake Baikal	Siberia	N-51°40' E-103°45'	0	*S. hangoei*	SHB	(Annenkova et al., 2015)
Listvyanka Lake Baikal	Siberia	N-51°49' E-104°52'	0	*P. baicalense*	PB	(Annenkova et al., 2015)
Lake Erken	Sweden	N-59°25' E- 18°15'	0	*P. aciculiferum*	Erk	(Annenkova et al., 2015)
Lake Østre Anlæg ved Sølvtorvet	Denmark	N-55°69' E-12°58'	0	*P. aciculiferum*	Cop	

The Strains of *S. hangoei* from Lake Baikal were sampled at Sludyanka by Rengefors, Kremp & Annenkova and isolated by A. Kremp. The *P. baicalense* from Lake Baikal were sampled at Listvyanka by Annenkova. Lake Baikal is the oldest, deepest and largest lake (in volume) on earth with a maximum depth of 1636 m, an average depth of 731 m and a volume of 23 015 km^3 (Shimaraev et al., 1994). Lake Baikal is a freshwater lake located in Eastern Siberia, Russia and is >25 million years old though 0.15 to 3.5 Ma years ago the lake became extremely deep due to tectonic events (Mats et al., 2011). It's ice covered every year for 4 – 6 months (Shimaraev et al., 1994).

Exp. 1. Intra- and interspecific variations in morphology (Hypothesis 1)

This experiment was conducted to measure the morphological differences among and within morphospecies and between freshwater- and marine-brackish species. The freshwater species would obtain a morphology that reduces sinking rate, while the marine-brackish species would retain a spherical shape that increases sinking rate. For that unicellular cultures of four different lineages, the marine-brackish species *S. hangoei* and *S.* aff. *hangoei* and the freshwater species *P. aciculiferum* and *P. baicalense* were compared. The cultures were kept in an incubator at 4 ±1°C, 50 µmol photons m^{-2} s^{-1} and 12:12 light/dark cycle. In total 8 populations from 7 different sampling sites were analysed (table 1). From each population of *S. hangoei* and *P. aciculiferum* 10 strains were selected to set up the experiment. For *S. hangoei*, strain no. 44, 127, 132, 134, 135, 136, 181, T35, T39 and T40 from Lake Abraxas (Abra), strain no. 109, 161, 190, 205, 207, 208, 209, 210, 221 and T7 from Lake McNeil (McNeil), strain no. 906, 908, 909, 912, 913, 914, 916, 918, 919 and 922 from Tvärminne (SHTV), strain no. 1301, 1303, 1304, 1305, 1306, 1308, 1310, 1311, 1318 and 1321 from the Gulf of Finland (SHLL7), strain no. 02, 07, 08, 09, 11, 12, 14, 15, 16 and 17 for Lake Baikal (SHB). For *P. aciculiferum*, strain no. 1, 1B, 2, 2B, 3B, 4, 5, 6, 8 and 16B from Lake Erken (Erk), strain no. 1, 2, 3, 6, 7, 8, 9, 10, 13 and 14 from Copenhagen (Cop). For *P. baicalense* only one strain was available, strain no. PB2-202.

Experimental set up

The freshwater species were cultured in modified Woods Hole (MWC) medium (salinity 0) based on Milli-Q water (Millipore Corp., Bedford, MA, USA) and the marine-brackish species were grown in 25 % seawater enriched with f/2 nutrient (Guillard and Ryther, 1962) to gain a salinity of ~7. The seawater was collected from the Öresund region of the Baltic Sea. All cultures were grown in 40 ml Nunc flasks with a starting concentration of 4000 cells ml^{-1} per strain at the culture conditions listed above. Four till five 1ml subsamples of each strain were taken to perform cell counts starting at day 7 until all strains reached stationary phase after 17 or 22 days. All subsamples were counted directly without fixation by using the Trigger Mode of the FlowCAM® (10x objective, FC100). The strains of *S. hangoei* from Lake Baikal were received from A. Kremp as samples fixed with Lugol's solution and thus counted with the Auto Image Mode of the FlowCAM® (10x objective, FC100). Growth rate (µ)

was calculated with strains in exponential phase as: $\mu = \ln(N2/N1)/(T2-T1)$ where N2 and N1 is the number of cells at time point 2 (T2) and time point 1 (T1) respectively.

The subsamples of strains in exponential growth were used to measure the fine-scale morphology by using the software VisualSpreadsheet®. From each strain the particle properties of 400 cells photographed in ventral or dorsal position and in focus were selected by applying population specific VisualSpreadsheet® filters. The particle property edge gradient was used to select cells in focus. To select cells in ventral and dorsal position circle fit and compactness was applied and saved as Classification in the VisualSpreadsheet® file.

Particle properties

The particle properties used for statistical analysis were aspect ratio, circle fit, diameter ESD, length, width, surface area to volume ratio, surface area and volume.

The aspect ratio is the ratio of the axis lengths of a particles Legendre ellipse of inertia (Figure 1). Particles which have a circular or quadratic shape have a value of 1. aspect ratio values close to zero are for long and thin particles. The circle fit is described as the deviation of the edge of the particle from a best-fit circle (Figure 1). The circle fit value of 1 is for particles with a shape of a perfect circle and values near zero are for particles that are not at all circular. (FlowCAM® Manual Version 3.4, 2014)

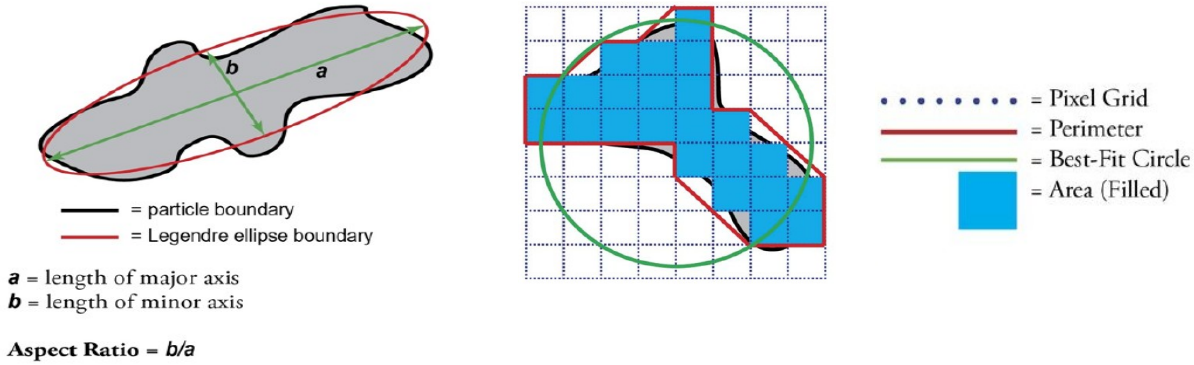

Figure 1: Illustration of the particle properties aspect ratio (left) and circle fit (right), FlowCAM® Manual Version 3.4, 2014

The diameter (ESD) is the Equivalent Spherical diameter and determined by the mean value of 36 feret measurements. The length is the maximum value and the width is the minimum value of 36 feret measurements. The Feret Measurement is the perpendicular distance between parallel tangents touching opposite sides of the particle (Figure 2). The VisualSpreadsheet® software makes 36

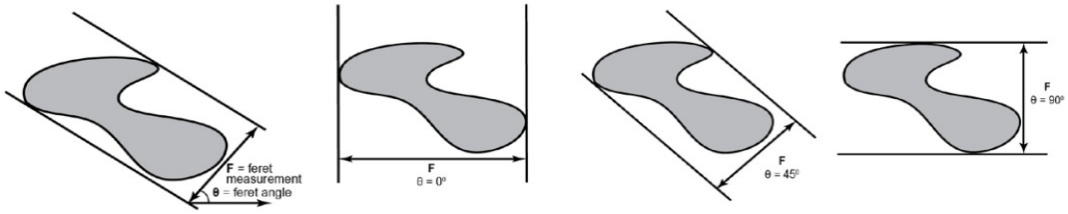

Figure 2: Examples of the Feret Measurement by the VisualSpreadsheet® software (FlowCAM® Manual Version 3.4, 2014)

measurements every 5 degrees for each particle. (FlowCAM® Manual Version 3.4, 2014)

The surface area and volume were calculated according to the equations of Sun, 2003. For the populations of the *P. aciculiferum* and the *P. baicalense* morphospecies the geometric shape of an ellipsoid with elliptic cross section was used. The formula of the geometric shape of a sphere was applied on the populations of the *S. hangoei* morphospecies. An R script was created to perform the calculations:

$$V_{sphere} = \frac{\pi}{6} \cdot a^3 \qquad V_{ellipsoid} = \frac{\pi}{6} \cdot a \cdot b \cdot c$$

$$A_{sphere} = \pi \cdot a^2 \qquad A_{ellipsoid} \approx \frac{\pi}{4} \cdot (b+c) \cdot \left[\left(\frac{b+c}{2} \right) + \frac{2a^2}{\sqrt{4a^2 - (b+c)^2}} \sin^{-1} \sqrt{\frac{4a^2 - (b+c)^2}{2a}} \right]$$

where a is length, b is width and c is Height of the cell.

The height of the *P. aciculiferum* and *P. baicalense* populations for the ellipsoid first had to be calculated. For the morphology analysis only 400 cells in ventral and dorsal position were manually selected so it was not possible to measure the height of the cells directly. Therefore 20 cells of each strain were manually selected which were pictured from the side so the height was visible and could be measured by the VisualSpreadsheet®. From the 20 height measurements of each strain a mean height to width ratio (f_{PA}) per strain for the *P. aciculiferum* populations and a mean height to length ratio (f_{PB}) per strain for the *P. baicalense* population was calculated. The height of the 400 cells per strain of the morphology measurements was then calculated by multiplying the width or the length with the ratio f_{PA} or f_{PB} respectively. $f_{PA} = height/width$ $f_{PB} = height/length$

Data analysis

The morphological differences within and among populations were tested by applying one-way analysis of variance, one-way ANOVA. Due to non equal variances within populations a one-way analysis of means, a Welch-test was performed. To test all shape parameters for main and interaction effects among morphospecies and original salinities (freshwater or marine-brackish species) two-way analysis of variance, two-way MANOVA, was used. The dependent variables were square root or log transformed if needed to meet the assumption of ANOVA. For all morphological and statistical analysis the software R (version 3.2.3, RStudio 0.99.491) was used.

Exp. 2. Sinking rates (Hypothesis 1)

This experiment was conducted to measure the sinking rates of non-motile (narcotised) cells (see method Nicotine solution treatment below) in freshwater by utilizing the FlowCAM method. The freshwater species would obtain a morphology that reduces sinking rate, while the marine-brackish species would retain a spherical shape that increases sinking rate. To measure the sinking rates one population of each morphospecies was chosen. 10 strains of Lake Erken (Erk) for *P. aciculiferum*, strain no. 1, 1B, 2, 2B, 3B, 4, 5, 6, 7 and 8 and 10 strains of Tvärminne (SHTV) for *S. hangoei*, strain

no. 908, 909, 913, 914, 916, 919, 901, 921, 1006 and 1008 were selected. For *P. baicalense* strain no. PB2-202 was used.

Experimental set up

The cultures in stationary phase set up for the competition experiment were used and diluted to initiate exponential growth. For that purpose culture was removed from each strain until ~5 ml was left and the culture flasks were filled up with medium to a total volume of 40 ml. Due to bad growth, new cultures were set up of the strains no. 7 and 8 of Erk after 20 days and strains no. 901, 921, 1006 and 1008 of SHTV after 14 days by transferring a 5 ml inoculum to 35 ml fresh medium. All cultures were grown under the same conditions as for the morphology experiment. All strains were cultured in modified Woods Hole medium (salinity 0) based on Milli-Q water (Millipore Corp., Bedford, MA, USA). To determine when the cultures reach exponential growth phase and to calculate the growth rate, cell counts were performed every 3 – 5 days after inoculation. Sinking rates were measured on strains in exponential growth.

The sinking rate measurements were carried out according to the method of Bach et al., 2012. The pump was disabled and the lower tube of the flow cell was closed airtight with a clip. After closing the tube 1 ml of MWC medium, followed by 200 µl nicotine solution and 1ml of sample was added into the pipette tip of the FlowCAM® and mixed shortly with the pipette. Then the tube was opened until the fluid reached the lower tube and then closed again. To measure the particles while sinking, the Auto Image Mode of VisualSpreadsheet® was selected (Appendix figure 14). Measurements were performed with the FlowCAM® by using a 10x objective and FC300 flow cell (300 µm depth, 3000 µm width). The FlowCAM®, nicotine solution (to narcotise cells, see below) and the MWC medium used for the measurements was put into a 10°C temperature controlled room for at least 15 min before measuring. The measurement was stopped after 20 min with *S. hangoei* strains and after 30 – 40 min with *P. aciculiferum* and *P. baicalense* strains.

Nicotine solution treatment

A nicotine solution was used to narcotise the algal cells and inhibit swimming without causing detectable damage to the cells. The solution was prepared according to Kamykowski et al., 1992. Five used menthol cigarette filters were cut into small pieces directly into a 30 ml glass bottle. Then 20 ml of MWC medium was added into the bottle, mixed, closed and stored overnight in the fridge. After 24 h the nicotine solution was filtered through a GF/F Whatman filter into an Erlenmeyer flask, was closed with an aluminium foil and stored until use in the fridge.

Narcotisation experiment

Prior to the sinking rate measurements, the optimal volume of nicotine solution needed to narcotise but not kill the cells was determined by conducting a narcotisation experiment. The experiment was carried out on live and killed cells. Dead cells were detected by using SYTOX® (30 µM) Green Dead Cell Stain (Invitrogen Ltd., Paisley, UK) which stains the nucleic acids of dead cells. The stain only

penetrates cells with compromised plasma membranes and when excited with 450 – 490 nm laser source the cells fluoresce bright green. Four different strains were selected: strain no. Erk6, SHTV908, Abra134 and PB2-202. Three different volumes of nicotine solution (25µl, 50µl and 100µl), two live cell controls and one dead cell control (150 µl of 95 % Ethanol) was set up for each strain. For that 6 x 1 ml of each strain was pipetted into a transparent microwell plate. Then the previously filtered nicotine solution and Ethanol was added. To all 1 ml samples 2µl of SYTOX green stain (30µM stock) was added to obtain a final concentration (M_f) of 0.05 – 0.06 µM (Appendix, Table 12). Immediately after adding SYTOX green the microwell plate was wrapped in aluminium foil and stored for 20 min in the dark at 4±1°C. After incubation each sample was checked for dead (fluorescence), live (motile) and narcotised (immotile, non fluorescence) cells in an inverted epifluorescence microscope (Nikon Eclipse TS100) by switching between fluorescent (488nm filter) and bright modes of the microscope.

Data analysis

To calculate the sinking velocities the MATLAB (MathWorks®) script of Bach et al., 2012 was applied. The MATLAB script was integrated into an R script which automatically imported all the exported VisualSpreadsheet® files and run the MATLAB script calculations. The MATLAB script used the particle properties saved by the VisualSpreadsheet® to automatically identify identical particles (Table 2) of each trajectory (see Appendix figure Fehler: Referenz nicht gefunden) and to calculate the sinking velocities. The strain Erk8 was excluded for sinking rate calculations due to low cell density. Some particle properties were defined as criteria in the MATLAB script which had to be fulfilled otherwise the particles would be excluded for further calculations. The edge gradient was set to a minimum of 130 for Erk and SHTV strains and 80 for PB2-202, to exclude particles not in focus. The diameter ESD were set to 10 as lower and 100 as upper boundary. The minimum required R-square of sinking particle fit was set to 0.95. The Y-axis upper starting point was set to 900 and the lower end point was set to 5 (in pixels). The minimum number of points needed in fit was 20 and the FlowCAM calibration factor was 0.5544. The sinking chamber diameter was 3000 µm with a sinking chamber factor of 1.004.

Table 2: MATLAB results per strain showing the number of particles identified as identical in each line (trajectory) by the MATLAB script and the total number of particles counted after excluding particles not in focus (edge gradient).

Strain	Nr. of particles identified as identical	total Nr. of particles counted	Strain	Nr. of particles identified as identical	total Nr. of particles counted
PB2-202	12	4899	SHTV908	10	3276
Erk1	13	1843	SHTV909	46	5774
Erk1B	9	7000	SHTV913	9	1920
Erk2	19	3581	SHTV914	17	7000
Erk2B	2	302	SHTV916	8	3126
Erk3B	12	5269	SHTV919	8	3157
Erk4	7	2004	SHTV901	9	4469
Erk5	28	10767	SHTV921	22	7000
Erk6	4	677	SHTV1006	21	7003
Erk7	4	916	SHTV1008	21	7000
Sum Erk	98	32359	Sum SHTV	171	49725

The particle properties surface area to volume ratio, surface area and volume were calculated with the same formulas as for the morphology experiment. Differences within and among populations in sinking

velocity (m d^{-1}), surface area to volume ratio and diameter ESD were tested by applying one-way analysis of variance, one-way ANOVA. The dependent variables were square root or log transformed if needed to meet the assumption of ANOVA. For statistical analysis and properties calculations the software R (version 3.2.3, RStudio 0.99.491) was used.

Exp. 3. Competition experiment (Hypothesis 2)

To set up the competition experiment 10 strains of *P. aciculiferum* from Lake Erken and *S. hangoei* from the Tvärminne location in the Baltic Sea were selected. For *S. hangoei*, these were strains no 901, 908, 909, 913, 914, 916, 919, 921, 1006 and 1008 of Tvärminne (SHTV). For *P. aciculiferum*, strains no. 1, 1B, 2, 2B, 3B, 4, 5, 6, 7 and 8 from Lake Erken (Erk) were used. The strains no 908, 909, 913, 914, 916, 919 of SHTV and 1, 1B, 2, 2B, 3B, 4, 5, 6, of Erk were inoculated already 82 days and strains no. 901, 921, 1006, 1008 of SHTV and 7, 8 of Erk were inoculated 20 days before starting the competition experiment. These single strain cultures were kept as back up cultures in an incubator at 4 ±1°C, 50 µmol photons m^{-2} s^{-1} and 12:12 light/dark cycle. The FlowCAM Auto Image Mode was used for all cell counts.

Experimental set up

The two species were allowed to compete under constant (CL) and fluctuating (FL) light conditions. Both light conditions were kept in the same incubator at 4 ±1°C with a light intensity of 50 µmol photons m^{-2} s^{-1} and 12:12 light/dark cycle. For the fluctuating light the light period (12h) was divided into 3 light and 2 dark cycles each turn with a duration of 144 min. The fluctuating light was set to medium frequency to simulate vertical mixing. For the fluctuating light set up the light installation was enclosed lightproof with four black plastic bags to ensure no external light source contamination of the experiment.

For each light condition five replicates, one *P. aciculiferum* FlowCAM Filter Control (Erk-filter-control) and one *S. hangoei* FlowCAM Filter Control (SHTV-filter-control) were set up. The Filter Controls were used to create VisualSpreadsheet® single species filters for each day. For each replicate 110 ml of MWC medium was inoculated with 20 ml of Erk-master-mix (*P. aciculiferum*) and 20 ml of SHTV-master-mix (*S. hangoei*) to obtain a total volume of 150 ml per replicate. The final cell concentration of each replicate was set to 4000 cells ml^{-1} including 2000 cells ml^{-1} of Erk-master-mix and 2000 cells ml^{-1} of SHTV-master-mix. For each Erk-filter-control 130 ml of MWC medium was inoculated with 20 ml of Erk-master-mix and for each SHTV-filter-control 130 ml of MWC medium was inoculated with 20 ml of SHTV-master-mix. The final cell concentration of each Filter Control was set to 2000 cells ml^{-1}.

The samples were taken at day 7, 10, 13, 16, 20, 22 and 26 after setting up the competition samples. From each replicate and filter control a 4 ml subsample was taken and immediately fixed with Lugol. Each subsample was measured 5 times with the Auto Image Mode of the FlowCAM. All subsamples

were taken during the light period of the fluctuating light between 17:36 – 20:00.

Master-mix preparation

The Erk-master-mix and the SHTV-master-mix were prepared shortly before inoculation. For that the 10 strains selected of *P. aciculiferum* were mixed to obtain the Erk-master-mix and the 10 strains selected of *S. hangoei* were mixed to obtain the SHTV-master-mix. For that each strain was counted to obtain the cell concentration and was added with equal cell concentration to the Erk-master-mix or SHTV-master-mix respectively. To add equal cell concentrations of each strain, the volume inoculum (Vi) was calculated per strain as:

$$V_{i.strain} = \frac{260\,ml \cdot \left(\frac{15000\,cells\,ml^{-1}}{10}\right)}{Cs_{strain}}$$

For the Erk-master-mix and the SHTV-master-mix the total volume (Vt) was set to 260 ml and the cell concentration (Cs) to 15 000 cells ml^{-1}. The cell concentration (Cs) for Erk-master-mix and SHTV-master-mix was calculated as:

$$Cs_{master\,mix} = \frac{150\,ml \cdot 2000\,cells\,ml^{-1}}{20\,ml}$$

Proportion analysis

The proportion experiment was set up together with the competition experiment by using the residue of the Erk-master-mix and the SHTV-master-mix. The proportion analysis was used to find out if the VisualSpreadsheet® species specific shape filters can determine the proportion of each species in a mixed sample with known proportion. Therefore I combined the Erk-master-mix and the SHTV-master-mix to obtain five samples of 3.5 ml with different proportions (10:90, 20:80, 50:50, 80:20 and 90:10) of each master-mix and a final cell concentration of 8000 cells ml^{-1} . Each master-mix was counted to obtain the cell concentration (Cs). The known cell concentration (Cs) was used to calculate the exact volume inoculum (V_i) of each master-mix to obtain the wanted proportion (Table 3) of each sample. Each sample was fixed with Lugol and counted five times with the Auto Image Mode of the FlowCAM. Each master-mix was also counted five times and used as filter control.

Table 3: Overview of the proportion mixes

Proportion Erk-master-mix	Proportion SHTV-master-mix	Cs Erk-master-mix (cells ml^{-1})	Cs SHTV-master-mix (cells ml^{-1})	V_i Erk-master-mix (ml)	V_i SHTV-master-mix (ml)	V_m MWC-medium (ml)	V_t sample (ml)
10	90	8319	10768	0.34	2.34	0.82	3.5
20	80	8319	10768	0.67	2.08	0.75	3.5
50	50	8319	10768	1.68	1.30	0.52	3.5
80	20	8319	10768	2.69	0.52	0.29	3.5
90	10	8319	10768	3.03	0.26	0.21	3.5

From the SHTV-master-mix counts a SHTV specific FlowCAM filter (SHTV-CAM-filter) was created. These SHTV-CAM-filter was first applied on the five Erk-master-mix and the five SHTV-master-mix counts to obtain the percentage these SHTV-CAM-filter can find in a pure Erk culture and a pure SHTV culture. The mean percentage of the SHTV-CAM-filter obtained from the five Erk-

master-mix counts was used as lower limit (42.6 %) and from the SHTV-master-mix as upper limit (61.9 %) to calculate the filter spread. The obtained filter spread was 19.3 and will be used in the extrapolation calculation for the proportion samples with the formula:

$$percentage\,extrapolated = \frac{(filtercount\ percentage * 100 - lower\ limit)}{filterspread}$$

The extrapolation was necessary because the SHTV-CAM-filter which should be specific for SHTV cultures only found ~60 % in pure SHTV culture and not 100% as expected. After applying the SHTV-CAM-filter on the proportion sample counts the received percentages of the SHTV-CAM-filter from each count were used in the extrapolation. A mean extrapolated percentage of the five counts from each proportion sample was calculated and plotted against the known proportion percentages (Figure 3). So the mean extrapolated percentage was compared with the known percentage of each proportion (Table 4) and can be used as reference for the extrapolated percentages obtained from each competition replicate (see Extrapolation set up).

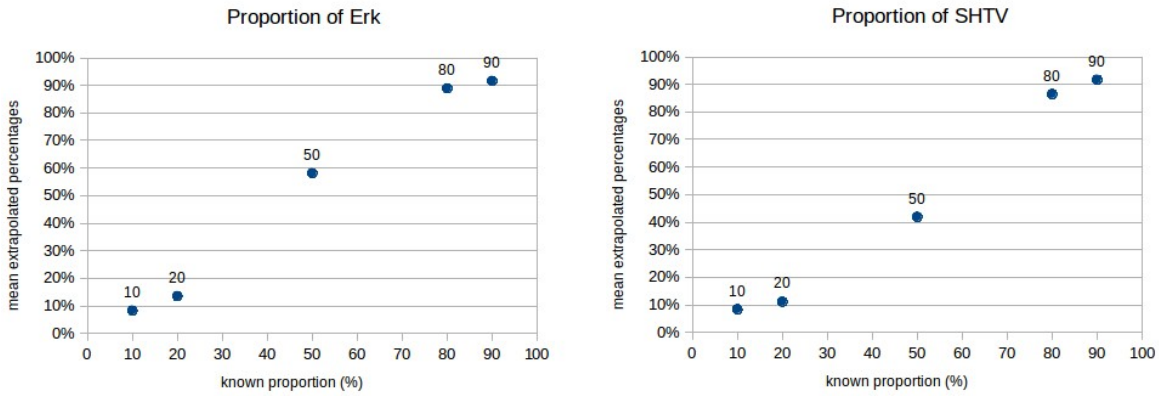

Figure 3: Mean extrapolated percentages of Erk (A) and SHTV (B) compared to the known proportion (%) after applying the SHTV-CAM-filter on each proportion sample

Table 4: Mean extrapolated and known proportion percentages of Erk and SHTV proportion samples including the reference values for 80 % (grey)

Mean extrapolated percentage Erk	% Known proportion Erk	Mean extrapolated percentage SHTV	% Known proportion SHTV
8%	10	92%	90
14%	20	86%	80
58%	50	42%	50
89%	80	11%	20
92%	90	8%	10

Extrapolation set up

Two species specific shape filters were created from the filter controls for each day and light condition separately. From each Erk-filter-control a species specific FlowCAM filter (Erk-CAM-filter) for the Erk population and from each SHTV-filter-control a species specific FlowCAM filter for the SHTV population (SHTV-CAM-filter) was created. For that the particle properties diameter ESD and circle fit were used. Both filters, Erk-CAM-filter and SHTV-CAM-filter were applied on the subsample measurements from replicates and filter controls of the corresponding day.

By applying the Erk- and SHTV-CAM-filter on the corresponding Erk- or SHTV-filter-controls the lower and upper limit was obtained which were used to calculate the filter spread for each day. By applying the Erk- and SHTV-CAM-filter on the replicates the number of cells the filters selected were used to calculate the filter count percentage for each filter seperately. Then the percentage of Erk and SHTV were extrapolated (see formula Proportion analysis) from each FlowCAM filter result and the mean extrapolated percentages from both filter results and for each population were calculated. The population which reached a extrapolated percentage of 80 % or more was defined as clear winning population. For the Erk population the corresponding 80 % were 89 % and for the SHTV population 86 % to be defined as clear winner (Table 4).

Data analysis

Differences in mean extrapolated percentages and mean cells ml^{-1} were tested among the light treatments and within each light treatment between the days and the replicates by applying one-way analysis of variance, one-way ANOVA. The dependent variables were square root or log transformed if needed to meet the assumption of ANOVA. For statistical analysis and properties calculations the programme R (version 3.2.3, RStudio 0.99.491) was used.

Results

Exp. 1. Intra- and interspecific variations in morphology (Hypothesis 1)

The comparison between populations and morphospecies of the different shape parameters are shown in Figure. 4 A-H). All populations are represented by 10 strains except for *P. baicalense* (PB2) represented only with one strain and excluded for ANOVA analysis among and within populations and among morphospecies but included in MANOVA among salinities. The MANOVA analysis tested among the two salinity categories, the freshwater and the marine-braskish species, showed that the marine-brackish species had a significantly higher mean aspect ratio ($F = 21.86$, d.f. = 1, $p < 0.01$) of 0.88 compared to the freshwater species with 0.78 and a higher mean circle fit ($F = 21.86$, d.f. = 1, $p < 0.01$) of 0.87 for the marine-brackish species compared to the freshwater species with 0.77 (Table 5). The marine-brackish species include the *S. hangoei* populations from Lake Abraxas (Abra), Lake McNeil (McNeil), Gulf of Finland (SHLL7) and Tvärminne (SHTV). The freshwater species include the *P. aciculiferum* populations from Denmark (Cop), Lake Erken (Erk) and Lake Baikal (PB2) and the *S. hangoei* population from Lake Baikal (SHB).

Statistical analysis showed significant differences among morphospecies. The *S. hangoei* morphospecies (SH) includes the populations from Lake Abraxas (Abra), Lake McNeil (McNeil), Gulf of Finland (SHLL7), Tvärminne (SHTV) and Lake Baikal (SHB). The *P. aciculiferum* morphospecies (PA) includes the populations from Denmark (Cop) and Lake Erken (Erk). The *S. hangoei* morphospecies was significantly higher in aspect ratio ($F = 16.42$, d.f. = 1, $p < 0.01$) and circle fit ($F = 23.97$, d.f. = 1, $p < 0.01$) than the *P. aciculiferum* morphospecies (Table 5). For the parameters diameter ESD ($F = 9.54$, d.f. = 1, $p < 0.05$) and length ($F = 35.65$, d.f. = 1, $p < 0.01$) the *P. aciculiferum* morphospecies showed significantly higher values than the *S. hangoei* morphospecies (Table 5). The morphospecies didn't differ significantly in width, surface area to volume ratio, surface area and volume ($F = 0.5$-2.34, d.f. = 1, $p = 0.19$-0.28).

There were highly significant differences within populations for all populations and for all variables tested, for the *P. aciculiferum* populations from Denmark (Cop, $F = 23.34$-279.81, $d.f._{(num)} = 9$, $d.f._{(denom)} = 1614.4$-1625.1, $p < 0.001$) and Lake Erken (Erk, $F = 30.61$-208.65, $d.f._{(num)} = 9$, $d.f._{(denom)} =$

Table 5: Summary of shape parameters per morphospecies and salinity groups

	Morphospecies			**Salinity groups**	
	S. hangoei	***P. aciculiferum***	***P. baicalense***	**Marine-brakish**	**Freshwater**
Aspect Ratio	0.87 (0.04)	0.76 (0.02)	0.79	0.88 (0.03)	0.78 (0.03)
Circle Fit	0.86 (0.03)	0.74 (0.02)	0.72	0.87 (0.03)	0.77 (0.04)
Diameter ESD (µm)	24.6 (1.8)	28.1 (0.9)	38.0	25.1 (1.3)	26.5 (3.6)
Length (µm)	26.6 (1.8)	33.1 (0.9)	43.5	27.1 (1.5)	30.6 (4.8)
Width (µm)	22.6 (1.9)	24.3 (1.0)	33.2	23.3 (1.3)	23.1 (3.0)
SA:V	0.26 (0.02)	0.25 (0.00)	0.19	0.25 (0.01)	0.26 (0.03)
Surface Area (µm²)	1813.1 (276.2)	2097.0 (148.1)	3554.5	1908.4 (211.2)	1929.4 (457.4)
Volume (µm³)	7331.6 (1650.9)	8702.6 (962.3)	18889.0	7885.5 (1312.8)	7874.3 (2791.0)

1591.1-1623.8, p < 0.001), for the *S. hangoei* population from the Gulf of Finland (SHLL7, F = 26.7-564.58, $d.f._{(num)}$ = 9, $d.f._{(denom)}$ = 1621.2-1625.4, p < 0.001), Tvärminne (SHTV, F = 29.41-181.54, $d.f._{(num)}$ = 9, $d.f._{(denom)}$ = 1622.9-1624.7, p < 0.001) and Lake Baikal (SHB, F = 38.09-120.59, $d.f._{(num)}$ = 9, $d.f._{(denom)}$ = 1617.6-1624.9, p < 0.001), for the *S.* aff. *hangoei* population from Lake Abraxas (Abra, F = 26.83-43.85, $d.f._{(num)}$ = 9, $d.f._{(denom)}$ = 1625.1-1625.4, p < 0.001) and from Lake McNeil (McNeil, F = 27.83-273.76, $d.f._{(num)}$ = 9, $d.f._{(denom)}$ = 1620.1-1624.7, p < 0.001).

The one-way ANOVA showed significant differences among populations with all variables tested, aspect ratio (F = 206.7, d.f. = 6, p < 0.001), circle fit (F = 191.4, d.f. = 6, p < 0.01), surface area to volume ratio (F = 23.22, d.f. = 6, p < 0.01), surface area (F = 24.17, d.f. = 6, p < 0.01), volume (F = 21.01, d.f. = 6, p < 0.01), diameter ESD (F = 37.22, d.f. = 6, p < 0.01), length (F = 77.41, d.f. = 6, p < 0.01) and width (F = 28.33, d.f. = 6, P<0.01). Overall there was no significant difference between the *P. aciculiferum* populations from Denmark (Cop) and Lake Erken (Erk) (TukeyHSD, p = 0.892-1.0) and between the Antarctic populations from Lake Abraxas (Abra) and from Lake McNeil (McNeil) (TukeyHSD, p = 0.810-0.999) among any tested shape parameters. The *S. hangoei* morphospecies with the population from Lake Baikal (SHB) differed significantly from all other populations among all shape parameters (TukeyHSD, p < 0.001, SHLL7:volume, diameterESD p < 0.05) except circle fit with the *S. hangoei* Baltic Sea population from Tvärminne (SHTV) (TukeyHSD, p =0.999) and length with the *S. hangoei* Baltic Sea population from the Gulf of Finland (SHLL7) (TukeyHSD, p = 0.186). The population *P. baicalense* from Lake Baikal (PB2) showed the highest values and the *S. hangoei* population from Lake Baikal (SHB) showed the lowest values in all shape parameters pictured (Table 6) except in the parameters aspect ratio, circle fit and SA:V ratio.

Table 6: Summary of shape parameters per population

Populations	Cop	Erk	PB2	SHB	Abra	McNeil	SHLL7	SHTV
Morphospecies	PA	PA	PB	SH	SH	SH	SH	SH
Aspect Ratio	0.76 (0.01)	0.76 (0.01)	0.79	0.82 (0.01)	0.91 (0.01)	0.91 (0.01)	0.87 (0.01)	0.85 (0.02)
Circle Fit	0.74 (0.05)	0.74 (0.04)	0.72	0.83 (0.04)	0.90 (0.04)	0.89 (0.04)	0.85 (0.04)	0.83 (0.04)
Diameter ESD (µm)	27.9 (1.9)	28.3 (2.3)	38.0	22.2 (2.4)	25.3 (2.0)	25.9 (2.3)	23.8 (1.8)	25.6 (2.2)
Length (µm)	33.0 (2.4)	33.1 (2.7)	43.5	24.5 (2.7)	26.9 (2.3)	27.4 (2.5)	25.8 (2.0)	28.3 (2.5)
Width (µm)	24.0 (2.0)	24.5 (2.2)	33.2	19.6 (2.3)	23.8 (2.0)	24.3 (2.3)	21.9 (1.9)	23.2 (2.2)
SA:V	0.25 (0.02)	0.24 (0.02)	0.19	0.29 (0.03)	0.24(0.02)	0.24 (0.02)	0.26 (0.02)	0.25 (0.02)
Surface Area (µm²)	2062 (303)	2132 (354)	3555	1432 (309)	1953 (319)	2028 (365)	1699 (272)	1953 (349)
Volume (µm³)	8453 (1917)	8953 (2280)	18889	5116 (1657)	8165 (1998)	8653 (2339)	6600 (1617)	8125 (2222)

The aspect ratio (Figure. 4 A) didn't differ significantly between the *P. aciculiferum* populations from Denmark (Cop) and Lake Erken (Erk) (TukeyHSD, p = 0.927) and between the Antarctic populations from Lake Abraxas (Abra) and Lake McNeil (McNeil) (TukeyHSD, p = 0.999). The *P. aciculiferum* populations from Denmark (Cop) and Lake Erken (Erk) had a significantly lower aspect ratio (TukeyHSD, p < 0.001) with 0.76 then all other populations (Table 6). The Antarctic populations from Lake Abraxas (Abra) and Lake McNeil (McNeil) had the highest aspect ratio with 0.91 and differed significantly (TukeyHSD, p < 0.001) from all other populations. The *S. hangoei* population from Lake Baikal (SHB), Gulf of Finland (SHLL7) and from Tvärminne (SHTV) differed significantly in aspect ratio from each other and from all other populations (TukeyHSD, SHLL7-SHB p < 0.001, SHTV-SHB and SHTV-SHLL7 p < 0.01).

The highest circle fit (Figure 4 B) was found in the Antarctic population from Lake Abraxas (Abra) with 0.9 followed by the Antarctic population from Lake McNeil (McNeil) with 0.89, the *S. hangoei* Baltic Sea population from the Gulf of Finland (SHLL7) with 0.85, the *S. hangoei* Baltic Sea population from Tvärminne (SHTV) with 0.83 and the *S. hangoei* population from Lake Baikal (SHB) with 0.83 (Table 6). The lowest values were attained by the *P. aciculiferum* populations from Denmark (Cop) and Lake Erken (Erk) with a circle fit of 0.74. These last two morphospecies (TukeyHSD, $p = 1.0$) showed a significantly lower (TukeyHSD, $p < 0.001$) circle fit compared with all other populations. The *S. hangoei* population from Lake Baikal (SHB) and the *S. hangoei* Baltic Sea population from Tvärminne (SHTV) (TukeyHSD, $p = 0.999$) showed a highly significantly smaller circle fit from the Antarctic populations from Lake Abraxas (Abra) and from Lake McNeil (McNeil) (TukeyHSD, $p < 0.001$) and a significantly lower circle fit from the *S. hangoei* Baltic Sea population from the Gulf of Finland (SHLL7) (TukeyHSD, $p < 0.05$). The Antarctic populations from Lake Abraxas (Abra) and from Lake McNeil (McNeil) (TukeyHSD, $p = 0.810$) had a significantly higher (TukeyHSD, $p < 0.001$) circle fit compared with all other populations.

The *P. baicalense* morphospecies from Lake Baikal (PB2) showed the largest diameter ESD with 38 µm (Figure 4 C) followed by the *P. aciculiferum* populations from Denmark (Cop) and Lake Erken (Erk) (TukeyHSD, $p = 0.969$) with 27.9 µm and 28.3 µm respectively (Table 6). The *P. aciculiferum* populations from Denmark (Cop) and Lake Erken (Erk) showed a significantly larger diameter compared to all other populations (TukeyHSD, $p < 0.001$, Cop:McNeil $p < 0.05$). The *S.* aff. *hangoei* morphospecies with the Antarctic populations from Lake Abraxas (Abra) and from Lake McNeil (McNeil) and the *S. hangoei* Baltic Sea population from Tvärminne (SHTV) (TukeyHSD, $p = 0.936$-0.999) showed a similar diameter between 25.3-25.9 µm. The *S. hangoei* population from Lake Baikal (SHB) obtained the smallest diameter with 22.2 µm followed by the *S. hangoei* Baltic Sea population from the Gulf of Finland (SHLL7) with 23.8 µm. The diameter of the *S. hangoei* population from Lake Baikal (SHB) was highly significantly smaller than all other populations (TukeyHSD, $p < 0.001$) and significantly smaller from the *S. hangoei* Baltic Sea population from the Gulf of Finland (SHLL7) (TukeyHSD, $p < 0.05$). The Gulf of Finland population (SHLL7) was also highly significantly smaller than the *P. aciculiferum* populations from Denmark (Cop) and Lake Erken (Erk) (TukeyHSD, $p < 0.001$) and significantly smaller than the Antarctic populations from Lake Abraxas (Abra) and from Lake McNeil (McNeil) and the *S. hangoei* Baltic Sea population from Tvärminne (SHTV) (TukeyHSD, $p < 0.05$).

The largest value of the length (Figure. 4 D) with 43.5 µm was obtained by the *P. baicalense* morphospecies from Lake Baikal (PB2) followed by the *P. aciculiferum* populations from Denmark (Cop) and Lake Erken (Erk) (TukeyHSD, $p = 0.999$) with 33 µm and 33.1 µm respectively (Table 6). The *P. aciculiferum* populations from Denmark (Cop) and Lake Erken (Erk) showed a significantly larger length than all other populations (TukeyHSD, $p < 0.001$). The *S. hangoei* Baltic Sea population

from Tvärminne (SHTV), the Antarctic populations from Lake Abraxas (Abra) and from Lake McNeil (McNeil) (TukeyHSD, p = 0.176-0.976) showed a similar length between 26.9-28.3 µm. The *S. hangoei* population from Lake Baikal (SHB) and the *S. hangoei* Baltic Sea population from the Gulf of Finland (SHLL7) obtained the smallest length of 24.5 µm and 25.8 µm respectively. The *S. hangoei* population from Lake Baikal (SHB) was highly significantly smaller in length (TukeyHSD, $p < 0.001$) compared to all other populations except the *S. hangoei* Baltic Sea population from the Gulf of Finland (SHLL7) (TukeyHSD, p = 0.186). The *S. hangoei* Baltic Sea population from the Gulf of Finland (SHLL7) was significantly smaller than the *P. aciculiferum* populations from Denmark (Cop) and Lake Erken (Erk) and the *S. hangoei* Baltic Sea population from Tvärminne (SHTV) (TukeyHSD, $p < 0.001$) and did not differ significantly from the Antarctic populations from Lake Abraxas (Abra) and from Lake McNeil (McNeil) and the *S. hangoei* population from Lake Baikal (SHB) (TukeyHSD, p = 0.088-0.456).

The largest width (Figure 4 E) was obtained by the *P. baicalense* morphospecies from Lake Baikal (PB2) with 33.2 µm. The *P. aciculiferum* populations from Denmark (Cop) and Lake Erken (Erk), the Antarctic populations from Lake Abraxas (Abra) and from Lake McNeil (McNeil) and the *S. hangoei* Baltic Sea population from Tvärminne (SHTV) were showing similar values ranging from 23.2-24.5 µm (Table 6) and didn't present significant differences (TukeyHSD, p = 0.079-0.999). They showed a significantly larger width than the *S. hangoei* population from Lake Baikal (SHB) and the *S. hangoei* Baltic Sea population from the Gulf of Finland (SHLL7) (TukeyHSD, $p < 0.001$) except the Tvärminne population (SHTV) with the Gulf of Finland population (SHLL7) (TukeyHSD, p = 0.097). The *S. hangoei* population from Lake Baikal (SHB) and the *S. hangoei* Baltic Sea population from the Gulf of Finland (SHLL7) obtained the smallest values with a width of 19.6 µm and 21.9 µm respectively. The *S. hangoei* population from Lake Baikal (SHB) had a significantly smaller width then the *S. hangoei* Baltic Sea population from the Gulf of Finland (SHLL7) (TukeyHSD, $p < 0.01$).

The surface area to volume ratio (SA:V) was highest for the *S. hangoei* morphospecies from Lake Baikal (SHB) with 0.29, followed by the *S. hangoei* morphospecies with the Baltic Sea population from the Gulf of Finland (SHLL7) and is shown in Figure 4 F. The *S. hangoei* morphospecies with the Baltic Sea population from Tvärminne (SHTV), the *P. aciculiferum* populations from Denmark (Cop) and Lake Erken (Erk) and the *S.* aff. *hangoei* morphospecies with the Antarctic populations from Lake Abraxas (Abra) and from Lake McNeil (McNeil) did not differ significantly and showed a SA:V ratio between 0.24-0.25 (Table 6). The *P. baicalense* morphospecies from Lake Baikal (PB2) showed the lowest ratio with 0.19. The SA:V ratio of *S. hangoei* morphospecies with the Baltic Sea population from the Gulf of Finland SHLL7 was significantly higher than the *S. hangoei* population from Tvärminne SHTV (TukeyHSD, $p < 0.05$) and highly significantly lower than the *S. hangoei* population from Lake Baikal (SHB) and highly significantly higher than all other populations (TukeyHSD, $p < 0.001$) except from the *P. aciculiferum* population from Denmark (Cop) (TukeyHSD, p = 0.091). The

S. hangoei population from Lake Baikal (SHB) was significantly higher in surface area to volume ratio than all other populations (TukeyHSD, $p < 0.001$).

The *P. baicalense* morphospecies from Lake Baikal (PB2) showed the largest surface area with 3555 µm² (Figure 4 G). The *S. hangoei* morphospecies with the Baltic Sea population from Tvärminne (SHTV), the *P. aciculiferum* populations from Denmark (Cop) and Lake Erken (Erk) and the *S.* aff. *hangoei* morphospecies with the Antarctic populations from Lake Abraxas (Abra) and from Lake McNeil (McNeil), obtained similar surface area values between 1953-2132 µm² and didn't differ significantly from each other (TukeyHSD, $p = 0.199$-1). The *S. hangoei* population from Lake Baikal (SHB) displayed the smallest surface area with 1432 µm² followed by the *S. hangoei* morphospecies with the Baltic Sea population from the Gulf of Finland (SHLL7) with 1699 µm² (Table 6). The surface area of the *S. hangoei* population from Lake Baikal (SHB) was highly significantly smaller than all other populations (TukeyHSD, $p = 0.001$) and significantly smaller from the *S. hangoei* population from the Gulf of Finland (SHLL7) (TukeyHSD, $p < 0.05$). The surface area of the *S. hangoei* population from the Gulf of Finland (SHLL7) was also highly significantly smaller than the *P. aciculiferum* populations from Denmark (Cop) and Lake Erken (Erk), the *S.* aff. *hangoei* morphospecies with the Antarctic population from Lake McNeil (McNeil) (TukeyHSD, $p < 0.001$) and significantly smaller than the *S.* aff. *hangoei* morphospecies with the Antarctic population from Lake Abraxas (Abra) and the Baltic Sea population from Tvärminne (SHTV) (TukeyHSD, $p < 0.05$).

Regarding the volume, the *P. baicalense* morphospecies from Lake Baikal (PB2) showed the largest value with 18889 µm³ (Figure 4 H). The populations display the same pattern as for the surface area. The *S. hangoei* morphospecies with the Baltic Sea population from Tvärminne (SHTV), the *P. aciculiferum* populations from Denmark (Cop) and Lake Erken (Erk) and the *S.* aff. *hangoei* morphospecies with the Antarctic populations from Lake Abraxas (Abra) and from Lake McNeil (McNeil) obtained similar volume values between 8125-8953 µm³ and did not differ significantly from each other (TukeyHSD, $p = 0.536$-1). The *S. hangoei* population from Lake Baikal (SHB) showed the smallest volume with 5116 µm³ followed by the Baltic Sea population from the Gulf of Finland (SHLL7) with 6600 µm² (Table 6). The volume of the *S. hangoei* population from Lake Baikal (SHB) was highly significantly smaller than all other populations (TukeyHSD, $p < 0.001$) and significantly smaller from SHLL7 (TukeyHSD, $p < 0.05$). The volume of the *S. hangoei* Baltic Sea population from the Gulf of Finland (SHLL7) was also highly significantly smaller than the *P. aciculiferum* population from Lake Erken (Erk), the *S.* aff. *hangoei* morphospecies with the Antarctic population from Lake McNeil (McNeil) (TukeyHSD, $p < 0.001$) and significantly smaller than the *P. aciculiferum* population from Denmark (Cop), the *S.* aff. *hangoei* morphospecies with the Antarctic population from Lake Abraxas (Abra) and the *S. hangoei* Baltic Sea population from Tvärminne (SHTV) (TukeyHSD, $p < 0.05$).

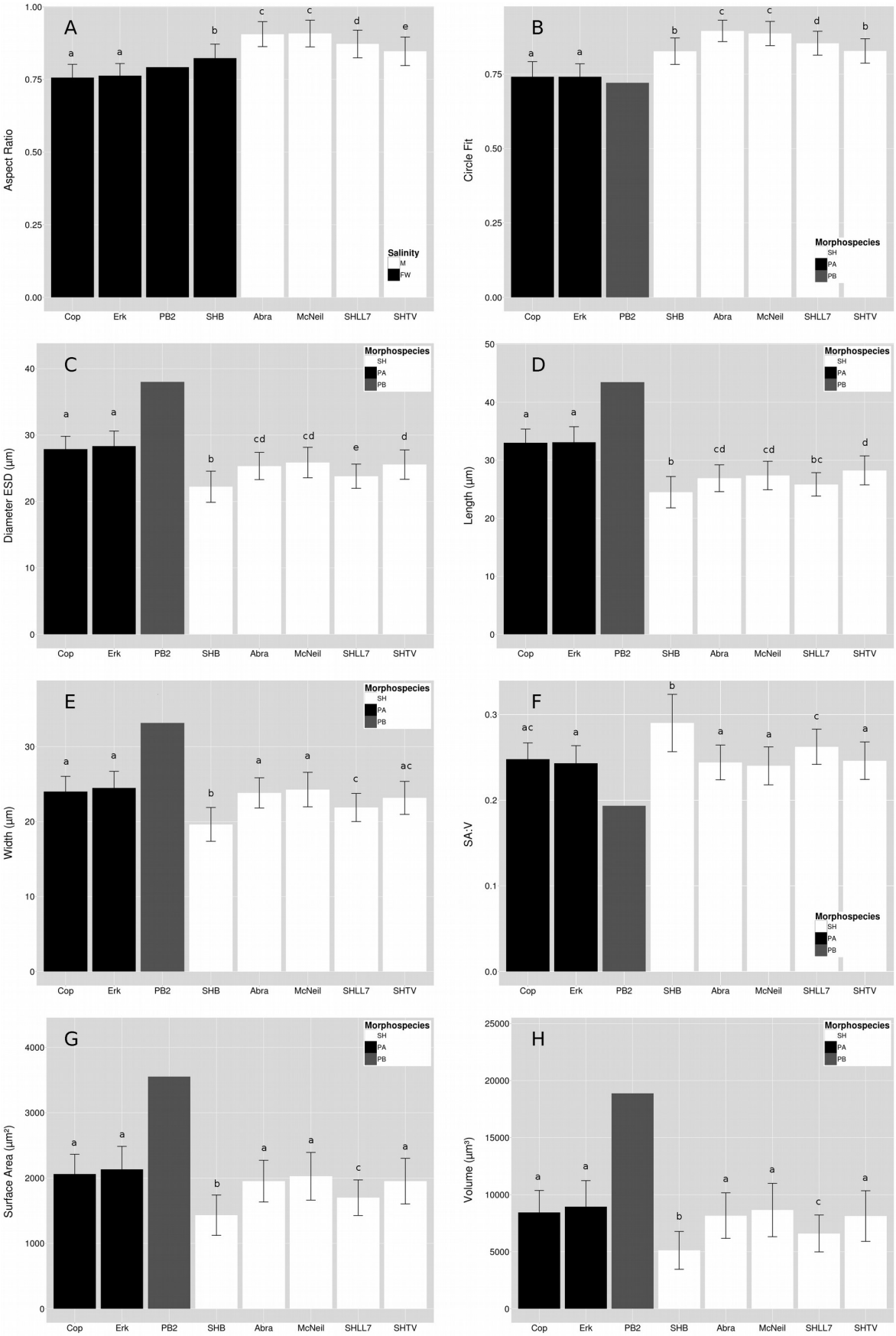

Figure 4: Comparison of shape parameters among populations in **A**-aspect ratio, **B**-circle fit, **C**-diameter ESD (µm), **D**-length (µm), **E**-width (µm), **F**-surface area to volume ratio (SA:V), **G**-surface area (µm²) and **H**-volume (µm³). Populations are ordered alphabetical from freshwater to marine-brakish species. Different letters indicate significant differences among populations (one-way ANOVA). Error bars represent standard errors.

The growth rate was calculated as mean growth rate over three time points during exponential growth. The marine-brackish populations were grown in salinity of ~7 and the freshwater species in salinity of 0. The highest mean growth rate was measured in the *P. baicalense* morphospecies from Lake Baikal (PB2) (0.20 divisions d^{-1}), followed by the *S. hangoei* Baltic Sea population from the Gulf of Finland (SHLL7) (0.18 divisions d^{-1}), the *S. hangoei* Baltic Sea population from Tvärminne (SHTV) (0.16 divisions d^{-1}) and the *P. aciculiferum* populations from Lake Erken (Erk) (0.15 divisions d^{-1}) (Figure 5 A). For the *P. baicalense* morphospecies from Lake Baikal (PB2) only one strain was in good growth and available. The lowest growth rates were measured in the *P. aciculiferum* populations from Denmark (Cop) (0.13 divisions d^{-1}), the Antarctic populations from Lake Abraxas (Abra) (0.12 divisions d^{-1}) and from Lake McNeil (McNeil) (0.12 divisions d^{-1}). Statistical analysis showed significant differences in mean growth rate among populations (one-way ANOVA, $F = 5.56$, $df = 5$, $p < 0.001$) and revealed a high variation of mean growth rates within each population, between strains. The *S. hangoei* Baltic Sea population from the Gulf of Finland (SHLL7) was significantly higher in mean growth rate than the *P. aciculiferum* population from Denmark (Cop) (TukeyHSD, $p < 0.05$), the Antarctic populations from Lake Abraxas (Abra) (TukeyHSD, $p < 0.001$) and Lake McNeil (McNeil) (TukeyHSD, $p < 0.001$).

The growth curve for each population is shown in Figure 5 B. The *S. hangoei* Baltic Sea population from the Gulf of Finland (SHLL7) and the *S. hangoei* Baltic Sea population from Tvärminne (SHTV) showed a steep increase in cell number and reached the highest number of cells after 18 days with 62014 cells ml^{-1} and 49825 cells ml^{-1} respectively. All populations reached stationary phase after 18 days except the Antarctic populations from Lake Abraxas (Abra) and the *S. hangoei* Baltic Sea population from Tvärminne (SHTV). The Antarctic populations from Lake Abraxas (Abra) showed a slow increase in cell number and the highest cell number was measured at day 23 with 6429 cells ml^{-1}. For the *S. hangoei* Baltic Sea population from Tvärminne (SHTV) no measurement was taken at day 23. The *P. aciculiferum* populations from Denmark (Cop) also slowly increased in cell number and

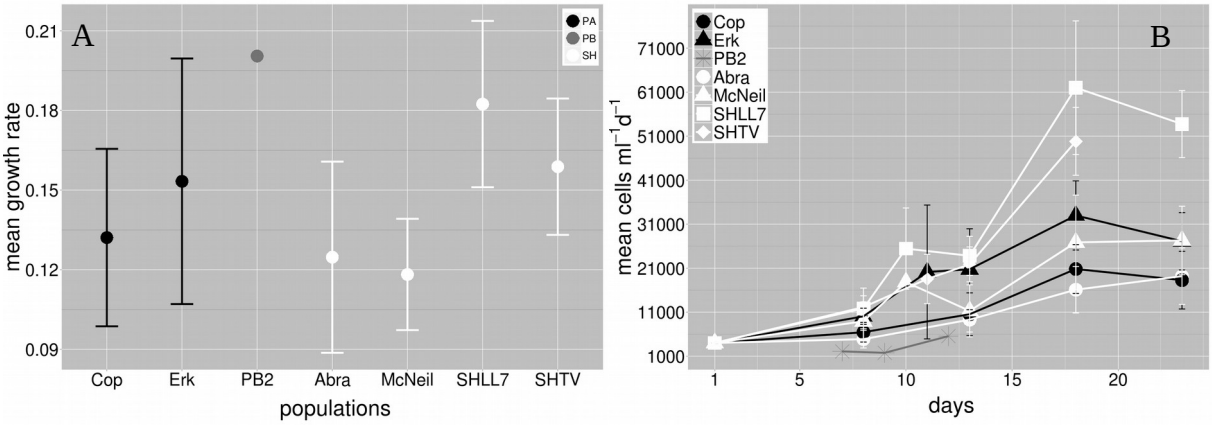

Figure 5: A- Mean growth rate per population, calculated over three time points during exponential growth. **B-** Mean number of cells ml^{-1} d^{-1}, measured on day 7, 10/11, 13, 18 and 23 for the populations Cop, Erk, Abra, McNeil, SHLL7 and SHTV and on day 7, 9 and 12 for the population PB2 (B). Error bars represent standard errors.

reached the maximum cell number at day 18 with 20812 cells ml^{-1}. The *P. aciculiferum* population from Lake Erken (Erk) and the Antarctic population from Lake McNeil (McNeil) had a sharp increase in cell number which was intermittent by a decrease in number of cells for the Antarctic populations from Lake McNeil (McNeil) at day 13. The *P. aciculiferum* populations from Lake Erken (Erk) and the Antarctic populations from Lake McNeil (McNeil) reached a maximum number of cells at day 18 with 32082 cells ml^{-1} and at day 23 with 27303 cells ml^{-1} respectively. The *P. baicalense* morphospecies from Lake Baikal (PB2) reached the highest number of cells after 12 days with 5544 cells ml^{-1}.

There was a significant slight linear relationship of growth rate with size for the *S. hangoei* morphospecies (Appendix, Figure 13). The P. aciculiferum morphospecies didn't show any significant linear relationship between mean growth rate and size. The linear regression between mean growth rate and circle fit (Y = 0.6349 (±0.1624) -0.5646 (±0.1874) X; r2 = 0.1927; F1, 38 = 9.071; p < 0.01) , diameter ESD (Y = 0.48134 (±0.10019) -0.01334 (±0.00398) X; r2 = 0.2282; F1, 38 = 11.23; p < 0.01) and width (Y = 0.523138 (±0.086317) -0.01618 (±0.003699) X; r2 = 0.3351; F1, 38 = 19.15; p < 0.001) showed a significant negative relationship for the *S. hangoei* morphospecies. The linear regression between mean growth rate and SA:V ratio (Y = -0.22319 (±0.09444) 1.48740 (±0.37988) X; r2 = 0.285; F1, 38 = 15.33; p < 0.001) was significant positive related for the *S. hangoei* morphospecies. The linear regression between mean growth rate and length was insignificant for both morphospecies.

Exp. 2. Sinking rates (Hypothesis 1)

The *P. baicalense* morphospecies from Lake Baikal (PB2) was excluded from all statistical analysis because only one strain was available. The one-way ANOVA showed a significant difference in sinking velocity (m d^{-1}) between strains within each population (Erk, F = 11.77, d.f. = 8, p < 0.001; SHTV, F = 39.71, d.f. = 9, p < 0.001). There was no significant difference in surface area to volume

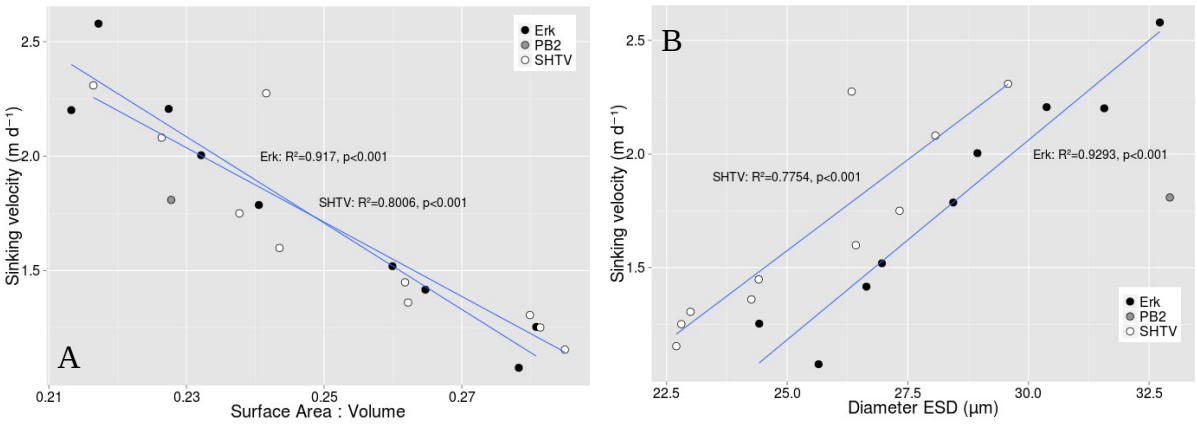

Figure 6: Linear regression between sinking velocity and surface area to volume ratio in **A** and between sinking velocity and diameter ESD (µm) in **B**. Each dot represents one strain.

ratio (one-way ANOVA, F = 0.439, d.f. = 1, p = 0.516) and in sinking velocity (m d^{-1}) among populations (one-way ANOVA, F = 0.29, d.f. = 1, p = 0.592). The diameter ESD (µm) showed significant differences among populations (one-way ANOVA, F = 6.075, d.f. = 1, p < 0.05).

The linear regression between sinking velocity and surface area to volume ratio (Figure 6 A) was highly significant for both populations, the *S. hangoei* Baltic Sea population from Tvärminne (Y = 5.770 (±0.678) -16.23 (±2.664) X; r2 = 0.823; F1, 8 = 37.13; p < 0.001) and the *P. aciculiferum* population from Lake Erken (Y = 6.422 (±0.493) -18.856 (±1.994) X; r2 = 0.927; F1, 7 = 89.39; p < 0.001). The linear regression between sinking velocity and diameter ESD (Figure. 6 B) was also highly significant for both populations, the *S. hangoei* Baltic Sea population from Tvärminne (Y = -2.422 (±0.723) + 0.159 (±0.028) X; r2 = 0.8004; F1, 8 = 32.08; p < 0.001) and the *P. aciculiferum* population from Lake Erken (Y = -3.205 (±0.486) + 0.176 (±0.017) X; r2 = 0.938; F1, 7 = 106.2; p < 0.001).The highest mean sinking velocity (m d^{-1}) was measured in the *P. baicalense* strain from Lake Baikal (PB2) with 1.81 m d^{-1} followed by the *P. aciculiferum* populations from Lake Erken (Erk) with 1.78 m d^{-1} and the *S. hangoei* Baltic Sea population from Tvärminne (SHTV) with 1.65 m d^{-1}. The highest mean diameter ESD (µm) was obtained by the *P. baicalense* strain from Lake Baikal (PB2) with 32.9 µm followed by the *P. aciculiferum* population from Lake Erken (Erk) with 28.4 µm and the *S. hangoei* Baltic Sea population from Tvärminne (SHTV) with 25.5 µm. For the surface area to volume ratio the highest value was calculated in the *S. hangoei* Baltic Sea population from Tvärminne (SHTV) with 0.254 followed by the *P. aciculiferum* population from Lake Erken (Erk) with 0.246 and the the *P. baicalense* strain from Lake Baikal (PB2) with 0.228. Statistical analysis showed no significant differences in mean growth rates (Figure 7) among populations (one-way ANOVA, F = 0.233, df = 1, p = 0.636). The highest mean growth rate was measured in the *P. baicalense* morphospecies from Lake Baikal (PB2) (0.20 divisions d^{-1}), followed by the *S. hangoei* Baltic Sea population from Tvärminne (SHTV) (0.15 divisions d^{-1}) and the *P. aciculiferum* population from Lake Erken (Erk) (0.12 divisions d^{-1}).

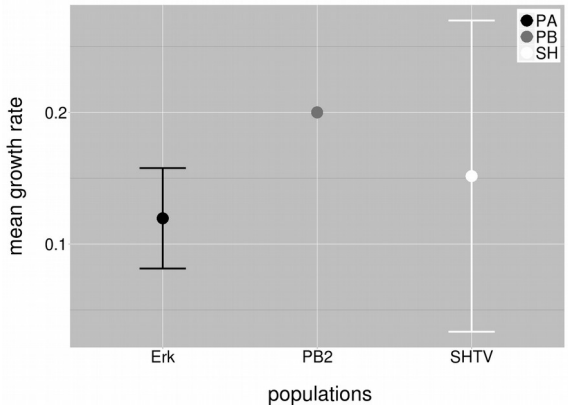

Figure 7: Mean growth rate per population of strains for sinking velocity measurements. Error bars indicate standard errors.

Exp. 3. Competition experiment (Hypothesis 2)

The *S. hangoei* Baltic Sea population from Tvärminne (SHTV) and the *P. aciculiferum* population from Lake Erken (Erk) were competing under constant (CL) and fluctuating (FL) light conditions. Each population is represented by 10 strains. The fluctuating light was used to simulate vertical mixing. The relative abundance of each population after extrapolation was calculated (Figure 8). The population gaining a relative abundance of 80 percent or more was defined as the winning population.
The one-way ANOVA showed no significant difference in mean percentages among the two light treatments (F = 1,581, d.f. = 1, p = 0.237) tested including all days and replicates. For the constant light, including all days and replicates, the *S. hangoei* Baltic Sea population from Tvärminne (SHTV) obtained a mean percentage of 55.7 % with the *P. aciculiferum* population from Lake Erken (Erk) obtaining a mean percentage of 44.3 %. For the fluctuating light, including all days and replicates, the *S. hangoei* Baltic Sea population from Tvärminne (SHTV) obtained a mean percentage of 67.1 % with the *P. aciculiferum* population from Lake Erken (Erk) obtaining a mean percentage of 32.9 %. There were significant differences of mean percentages among both light treatments at day 13 (one-way ANOVA, F = 17.26, d.f. =1, p < 0.01), 22 (one-way ANOVA, F = 19.21, d.f. =1, p < 0.01) and 26 (one-way ANOVA, F = 45.53, d.f. =1, p < 0.001) when tested for each day separately. For the days 7 (one-way ANOVA, F = 0.024, d.f. = 1, p = 0.882), 16 (one-way ANOVA, F = 2.325, d.f. = 1, p = 0.171) and 20 (one-way ANOVA, F = 4.164, d.f. = 1, p = 0.076) no significant differences were determined among the light treatments when tested for each day separately.

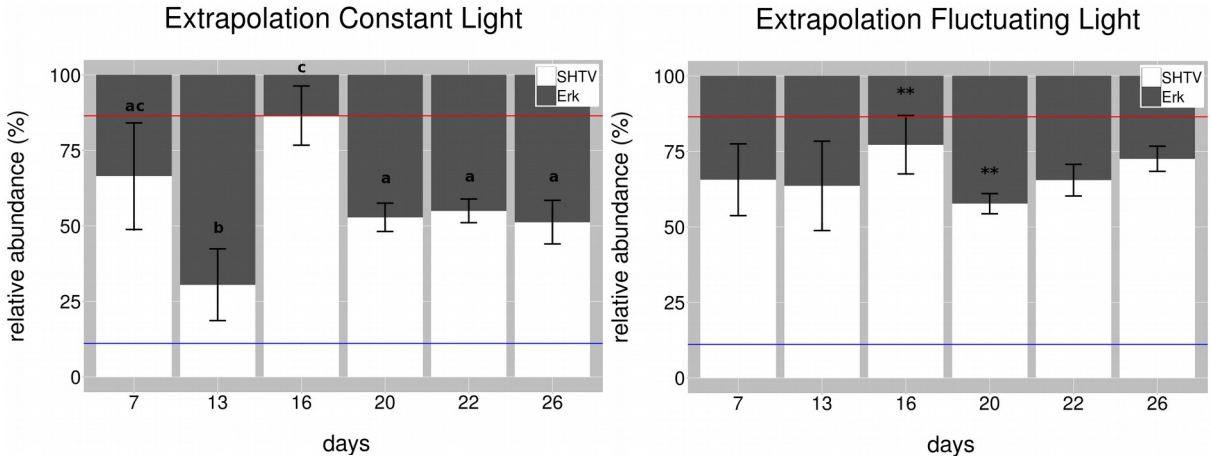

Figure 8: Relative abundance of populations in mixed competition cultures, extrapolated for day 7, 13, 16, 20, 22 and 26. Red line marks 80 % and blue line 20 % of relative abundance. Different letters and stars indicate significant differences in relative abundances among days (one-way ANOVA). Error bars represent standard errors.

There were significant differences in mean percentages among days including all five replicates when tested for each light condition separately, with the constant light (F = 16.63, d.f. = 5, p < 0.001) and the the fluctuating light (F = 3.869, d.f. = 5, p < 0.05). There was no significant difference in mean percentages among the replicates, tested for each light condition separately including all days with the constant light (one-way ANOVA, F = 0.059, d.f. = 4, p = 0.993) and with the fluctuating light (one-

way ANOVA, F = 1.429, d.f. = 4, p = 0.254). The one-way ANOVA showed significant differences in mean percentages among replicates when tested for each day separately with the constant light (day7: F =9.42, d.f. = 4, p < 0.001; day13: F = 14.69, d.f. = 4, p < 0.001; day16: F = 11.36, d.f. = 3, p < 0.01; day20: F = 64.84, d.f. = 4, p < 0.001; day22: F = 13.51, d.f. = 4, p < 0.001; day26: F = 9.528 , d.f. = 4, p < 0.001) and the fluctuating light (day13: F = 15.24, d.f. = 4, p < 0.001; day16: F = 6.708, d.f. = 4, p < 0.01; day22: F = 3.788, d.f. = 4, p < 0.05; day26: F = 3.183 , d.f. = 4, p < 0.05) except day 7 (F = 2.03, d.f. = 4, p = 0.129 and day 20 (F = 1.827, d.f. = 4, p = 0.163).

The *S. hangoei* Baltic Sea population from Tvärminne (SHTV) obtained the highest relative abundance with 87 % (Table 7) in constant light at day 16 and can be defined as clear winner (Figure 8). Day 16 under constant light the *S. hangoei* Baltic Sea population from Tvärminne (SHTV) was significantly higher than all other days (TukeyHSD, day20, 22 p < 0.01; day13, 26 p < 0.001) except day 7 (TukeyHSD, p = 0.105). Day 13 under constant light of the *P. aciculiferum* population from Lake Erken (Erk) was significantly higher with 69.5 % than all other days (TukeyHSD, day 20, 22, 26 p < 0.01; day 7, 16 p < 0.001). The percentages at the days 7, 20, 22 and 26 under constant light of the *S. hangoei* Baltic Sea population from Tvärminne (SHTV) were between 51.3 – 66.5 % (Table 7). The days 7, 20, 22 and 26 of the constant light didn't differ significantly (TukeyHSD, p = 0.094 – 0.999).
For the fluctuating light the mean percentage of the *S. hangoei* Baltic Sea population from Tvärminne (SHTV) of day 16 with 78.2 % was significantly higher than day 20 with 67.7 % (TukeyHSD, p < 0.01). The days 7, 13, 16, 20, 22 and 26 from the fluctuating light (Figure 8), except day 16 compared to day 20, didn't differ significantly (TukeyHSD, p = 0.064 – 0.988). The mean percentages at day 7, 13, 22, and 26 under fluctuating light of the *S. hangoei* Baltic Sea population from Tvärminne (SHTV) were between 63.7 – 72.5 %. The highest mean percentage of *P. aciculiferum* from Lake Erken (Erk) during constant light was 42.3 % at day 20.

Table 7: Relative abundance of SHTV and mean number of cells ml^{-1} for each day and light treatment.

Days	**7**	**13**	**16**	**20**	**22**	**26**
SHTV constant light (%)	66,5	30,5	87,1	52,9	55,0	51,3
SHTV fluctuating light (%)	66,5	63,7	78,2	57,7	65,5	72,5
Cells ml^{-1} constant light	4597	12760	14924	31543	38626	45239
Cells ml^{-1} fluctuating light	4373	10834	11062	15033	20630	26605

The growth curves of both light treatments show a constant increase in cell number (Figure 9). After 26 days of growth both light treatments didn't reach stationary phase. The one-way ANOVA showed no significant difference in mean cells per ml among the two light treatments (F = 1.781, d.f. = 1, p = 0.212) tested including all days and replicates. There was significant difference of mean cells per ml among both light treatments at day 20 (one-way ANOVA, F = 249.5, d.f. =1, p < 0.001), 22 (one-way ANOVA, F = 95.19, d.f. =1, p < 0.001) and 26 (one-way ANOVA, F = 19.5, d.f. =1, p < 0.001) when tested for each day separately. For the days 7 (one-way ANOVA, F = 0.034 d.f. = 1, p = 0.857), 13 (one-way ANOVA, F = 2.637, d.f. = 1, p = 0.143) and 16 (one-way ANOVA, F = 1.641, d.f. = 1, p =

0.241) no significant difference was determined among the light treatments when tested for each day separately. The one-way ANOVA showed no significant differences in mean cells per ml among replicates when tested for each day separately with the constant light for day 13 (F = 1.545, d.f. = 4, p = 0.237) and 20 (F= 0.14, d.f. = 4, p = 0.965) and with the fluctuating light for day 7 (F = 1.448, d.f. = 4, p = 0.255), 13 (F = 1.906, d.f. = 4, p = 0.149), 16 (F = 2.357, d.f. = 4, p = 0.092), 22 (F = 0.795, d.f. = 4, p = 0.542) and 26 (F = 2.179, d.f. = 4, p = 0.11). There was significant difference for day 7 (F = 11.55, d.f. = 4, p < 0.001), 16 (F = 36.49 , d.f. = 3, p < 0.001), 22 (F = 4.965, d.f. = 4, p < 0.01) and 26 (F = 7.659, d.f. = 4, p < 0.001) of constant light and for day 20 (F = 3.129, d.f. = 4, p < 0.05) of fluctuating light in mean cells per ml among replicates when tested for each day separately.

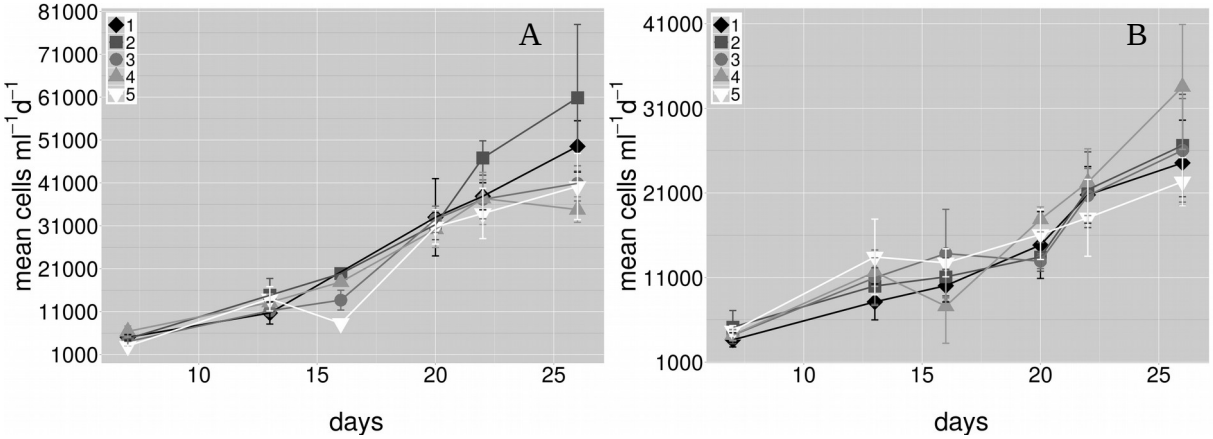

Figure 9: Growth curve of each replicate for the constant light (**A**) and the fluctuating light (**B**). Mean number of cells ml^{-1} d^{-1} were measured on day 7, 13, 16, 20, 22 and 26. Error bars represent standard errors.

Discussion

The cold-water species *Peridinium aciculiferum* and *Scrippsiella hangoei* form a species flock with small genetic differences but large distinct morphological differences. It has been hypothised that this species flock could be an example of a recent rapid adaptive radition in response to environmental changes such as salinity differences. Saline water has a higher density then fresh water and therefore the selection pressure on cell shape and size to remain suspended in the water, should be much higher in freshwater than in seawater. Therefore we would expect differences in morphology between the two environments. Studies from another cold-water dinoflagellates indicate local adaptation favoured by salinity differences (Rengefors et al., 2015). Here the fine-scale morphology and sinking velocity was studied in the cold-water *Peridinium aciculiferum* / *Scrippsiella hangoei* species flock. Furthermore the freshwater *Peridinium aciculiferum* and the marine-brackish *Scrippsiella hangoei* were competed under constant and fluctuating light conditions. The morphology experiment was conducted to measure the morphological differences among and within morphospecies and between freshwater- and marine-brackish species.

My objective was to determine weather the freshwater species have obtained a morphology that reduces sinking rate, while the marine-brackish species have retained a spherical shape that increases sinking rate. Further I hypothesised that the species adapted to vertical mixing will dominate under fluctuating light conditions (i. e. turbulent, not ice covered water), while the species adapted to non or horizontal movements will dominate under stable light conditions (stratified, ice covered water).

Intra- and interspecific variations in morphology and sinking rate

Here I tested the selective force of salinity on morphology by looking for intra- and interspecific morphological differences between the freshwater *P. aciculiferum* and marin-brackish *S. hangoei* species. These two species were also characterised as two different morphospecies. *S. hangoei* from the freshwater Lake Baikal was included in the *S. hangoei* morphospecies when tested among morphospecies. When tested among salinities, characterised as freshwater or marine-brackish species, *S. hangoei* and *P. baicalense* from Lake Baikal were counted as freshwater species. The results of the FlowCAM morphology analysis showed that there were significant differences among the morphospecies in aspect ratio, circle fit, diameter and length. Basically it confirms that these observed differences in morphology can be used to describe the obvious core differences in morphology that also can be detected by eye. The *P. aciculiferum* morphospecies is significantly larger in size and more elongated than the *S. hangoei* morphospecies (including *S. hangoei* from Lake Baikal) which obtained significantly higher values in aspect ratio and circle fit. These findings confirm the description of Logares et al. (2007a) that the *S. hangoei* morphospecies has a more circular shape than the *P. aciculiferum* morphospecies. However, the shape parameters SA:V, surface area, volume and width

didn't differ significantly among morphospecies. These shape parameters are important measurements in terms of sinking rate. In general it is agreed to that sinking rate is closely linked to a cell's surface area to volume ratio (SMAYDA, 1970). A larger cell size would increase the sinking velocity and a larger surface area to volume ratio would decrease the sinking velocity (Kamykowski et al., 1992). When tested among salinities only two shape parameters were significantly different. The marine-brackish species had significantly higher values in aspect ratio and circle fit, meaning that the marine-brackish species have a more circular shape than the freshwater species (including *S. hangoei* from Lake Baikal).

It is known that spines can increase the surface area and therefore decrease the sinking rate, but only if the density of the spines is exceeded by the corresponding increase in drag (Anderson et al., 1985). The study of *Scrippsiella trochoidea* cysts with short dense spines showed that spines can increase sinking rate compared to spineless cysts (Anderson et al., 1985). A study of the diatom *Thalassiosira fluviatilis* Hustedt showed that spines did affect the sinking rate because the length of the spines was several times the cell radius (Walsby and Xypolyta, 1977). In fact, for calculating the surface area and the volume of the *P. aciculiferum* species the spines couldn't be taken into account due to the resolution of the FlowCAM pictures, which was too low for this purpose. However, spines are an important measurement in terms of sinking rate and could increase the surface area and possibly decrease the sinking velocity (Anderson et al., 1985). Although in the sinking rate measurements the spines of *P. aciculiferum* are taken into account, the sinking rates didn't show significant differences among the morphospecies. Nevertheless, the sinking rate results showed a high within-species difference meaning that shape differences between strains are stronger than between species in terms of sinking velocity. The differences in sinking rates among strains are correlated to a high degree to the surface area to volume ratio and diameter. There is a strong negative correlation between sinking velocity and surface area to volume ratio and a strong positive correlation between sinking velocity and diameter. These findings confirm that the sinking rate increases with size and decreases with surface area to volume ratio. Contrary to expectations, the *S. hangoei* morphospecies obtained the lowest sinking rate and the highest surface area to volume ratio compared to the other morphospecies.

The tested shape differences don't coincide with freshwater species because the freshwater *S. hangoei* from Lake Baikal was significantly smaller in diameter, length, width, surface area and volume and significantly larger in aspect ratio, circle fit and SA:V ratio, from all other freshwater populations. The Baikal *S. hangoei* population was also significantly smaller from the other marine-brakish *S. hangoei* and *S. aff. hangoei* populations in aspect ratio, circle fit, diameter, length, width, surface area and volume and obtained the significantly highest SA:V ratio. Only in circle fit with the marine-brakish *S. hangoei* from Tvärminne and in length with the marine-brakish *S. hangoei* from the Gulf of Finland it didn't differ significantly. As the morphology of the baikal *S. hangoei* showed such significantly different values from all the other populations including the other *S. hangoei* and *S. aff. hangoei*

populations, except in two parameters from the Baltic Sea populations, maybe it is overall a distinct species and as cryptic species part of the *S. hangoei* complex. Annenkova et al., 2015 suggested that the *S. hangoei* morphospecies could include at least three cryptic species. The *P. baicalense* also showed a morphology different from all other populations, even though we couldn't test this statistically due to a lack of strains. However, we can't rule out that the *P. baicalense* morphospecies has a morphology that reduces sinking rate because only one strain was available. We also were not able to measure spine length and furthermore, in culture *P. baicalense* reduces the spines compared to field measurements (Annenkova et al., 2015). Ideally samples from the field should be measured directly by using the FlowCAM.

The intraspecific morphological differences were significant only within the *S. hangoei* morphospecies. The populations Lake Erken and Copenhagen from the *P. aciculiferum* morphospecies didn't show any significant morphological differences. Also the Antarctic *S.* aff. *hangoei* populations from Lake Abraxas and Lake McNeil didn't differ significantly in shape from each other and revealed to be the most circular populations of all populations tested. However, the Baltic populations from Tvärminne and the Gulf of Finland showed significant morphological differences from each other and from the other *S. hangoei* populations in most of the shape parameters. In general when comparing the marine-brackish *S. hangoei* populations, the populations from Tvärminne, Lake Abraxas and Lake McNeil were similar in diameter, length and width and significantly larger than the Gulf of Finland, Baltic Sea population. However, the Gulf of Finland population obtained the significantly smallest surface area and volume and therefore the significantly highest SA:V ratio compared to the other marine-brackish *S. hangoei* populations. The Gulf of Finland population was also more circular than the Tvärminne population. Overall the intraspecific morphological differences were higher within the marine-brackish *S. hangoei* morphospecies than within the freshwater P. aciculiferum morphospecies. This suggests that populations of the same morphospecies from sampling sites located closer to each other show a more similar morphology, due to gene flow among populations, as well as similar environments. Annenkova et al., 2015 already confirmed that there are small intraspecific genetic differences between the locations of the *S. hangoei* morphospecies. An explanation could be that in the *S. hangoei* morphospecies cryptic species occur or that the morphospecies is a single cosmopolitan species with isolated populations (Annenkova et al., 2015).

I have to reject my hypothesis that the freshwater morphospecies have a morphology that reduces the sinking rate, although I can confirm that the marine-brackish species have a more spherical morphology and the freshwater morphospecies *P. aciculiferum* is larger in size. The shape differences among the morphospecies do not seem to be caused by density differences, meaning that the morphology is not under strong selective pressure in terms of reducing the sinking velocity. This could be explained by the fact that these are swimming species and hence they are able to compensate sinking without paying a high metabolic cost. This suggests that instead the freshwater species could

have obtained a morphology which potentially enhances swimming efficiency. Kamykowski et al. (1992) confirmed that maximum swimming velocity is obtained with intermediate cell size for dinoflagellates with a standard propulsion system but swimming velocity also increases with cell length. Both morphospecies had a medium cell size with a diameter ESD of 25 µm and 28 µm for *S. hangoei* and *P. aciculiferum* respectively. However, in the *P. aciculiferum* morphospecies the length was significantly greater than in the *S. hangoei* morphospecies.

The swim to sink ratio (swim:sink) is an important measurement to determine how strongly sinking influences swimming velocity. The swim:sink ratio increased and the swimming velocity decreased with increasing surface area to volume ratio (Kamykowski et al., 1992). Also the swim:sink ratio decreased with increasing diameter ESD up to 25 µm and then stayed constant at a ratio of 7.6 (Kamykowski et al., 1992). Both morphospecies have a similar sinking rate and surface area to volume ratio but differ in cell size. The elongated shape of *P. aciculiferum* and the larger cell length could be a crucial factor to enhance the swimming velocity and increase the swim:sink ratio. Therefore further analysis would be necessary to determine swimming velocities of *P. aciculiferum* and *S. hangoei*. For that the FlowCAM could be set up as described in the sinking rate methods except without narcotising the cells.

Competition of *P. aciculiferum* and *S. hangoei* under constant and fluctuating light

Here I wanted to investigate why *S. hangoei* from the Baltic Sea doesn't occur in swedish freshwater lakes especially in Lake Erken, even though *S. hangoei* can grow in salinity ranging from 0 to 30 (Logares et al., 2008). Lake Erken is only ~15 km away from the Baltic sea (Logares et al., 2007a) and they are connected through a network of streams (Ekman and Fries, 1970), hence dispersal should be possible and geographical isolation must play a minor role (Annenkova et al., 2015). Therefore I competed *P. aciculiferum* from Lake Erken with *S. hangoei* from the Baltic Sea. I proposed that vertical mixing and fluctuating light conditions would be less important in Lake Erken than in the Baltic sea and thus *P. aciculiferum* would dominate under stable light conditions. *S. hangoei* could depend on vertical mixing to stay at the surface layers, due to morphological constraints which increase sinking.

There was no significant difference in relative abundance of *S. hangoei* and *P. aciculiferum* among the two light treatments. *S. hangoei* seemed to do slightly better in fluctuating light than in constant light with mean percentages of 67 % and 55 % of all cells respectively. *S. hangoei* reached the 80 % mark at day 16 of the total number of cells with the constant light, meaning that there is no advantage for *P. aciculiferum* growing under constant light. Consequently, I had to reject my hypothesis that *P. aciculiferum* will dominate under constant light conditions and hence can out compete *S. hangoei*. However, it is possible that *S. hangoei* in general grows better in culture than *P. aciculiferum*. The

mean growth rates of *S. hangoei* from the Baltic sea measured during the morphology and sinking rate experiments are always slightly higher than from the *P. aciculiferum* population from Lake Erken, although they are not significantly different. As the two species are competing for nutrients and light it could be possible that with increasing growth they decrease cell size to enhance nutrient uptake. Nielsen and Sand-Jensen (1990) confirmed the findings of Banse (1976) that there is a size dependence of growth among microalgae but it is lower than in other organisms. The regression analysis of the morphology populations showed that there was a slightly negative relationship between mean growth rate and circle fit, diameter ESD and width and a slightly positive relationship between mean growth rate and SA:V ratio for the *S. hangoei* morphospecies. This indicates that there is a size dependence of growth for the marine-brackish *S. hangoei* morphospecies.

The extrapolation method that I applied was not resistant against any morphological changes and changes in size. If the cultures in competition changes their size compared to the control cultures, the extrapolation would malfunction, resulting in a biased outcome probably beneficial to the smaller spherical *S. hangoei*.

Evaluation of the FlowCAM method

For all experiments the FlowCAM was used to determine morphology and cell density. The VisualSpreadsheet® automatically calculates the particle properties and the particles per ml for each run. Only a small sample volume (0.05 ml) was necessary for each run. It is a fast and quantitative method without any expensive or time consuming preparations necessary before each run, although it can happen that the flow cell clogs and cleaning the flow cell can be a time consuming process. Also, with the FlowCAM method it is possible to obtain a huge amount of data which need to be revised before they can be used in downstream analyses. This needs to be considered in the experimental set up beforehand.

Due to the relative small cell size of the species used (<40 µm) the 10x objective was not enough to capture the fine-scale morphology such as spines. For that I would suggest to use an objective with higher resolution. Also, by using the FC100 flow cell for cell counts the cell density is only an estimation by the VisualSpreadsheet® software. To obtain the exact number of cells for each run a field-of-view (FOV) flow cell would be a better choice.

Acknowledgements

First of all I would like to thank my supervisor Karin Rengefors for giving me the opportunity to be part of her working group and for all the fruitful discussions. Without her guidance this thesis wouldn't have been possible.

Many thanks to Marie Svensson and Helena Truong for their technical and laboratory support during my experimental time at the Algae Lab, Lund University. Also, many thanks to the Aquatic Ecology Unit, Department of Biology, Lund University for providing me with a great working environment and laboratory facilites. I thank Anke Kremp for supplying valualbe information and algae samples of *S. hangoei* from Lake Baikal.

I also would like to thank Michael Schagerl for taking the guiding mentor position and all his administrative support at the University of Vienna.

Big thanks to my colleagues and friends for sharing knowledge and time together and for always lending me a sympathic ear during my study period.

Lots of thanks to my family for trusting in me and my decisions, for being there for me and their great unquestionable support.

Finally I would love to thank my partner in life Nils Kalchhauser for his great support in all kinds of technical and mathematical questions and all the experiences we shared together; For his positive thoughts which always motivated me and for keeping me on track.

References

Anderson, D.M., Lively, J.J., Reardon, E.M., Price, C.A., 1985. Sinking characteristics of dinoflagellate cysts. Limnol. Oceanogr. 30, 1000–1009. doi:10.4319/lo.1985.30.5.1000

Annenkova, N.V., Hansen, G., Moestrup, Ø., Rengefors, K., 2015. Recent radiation in a marine and freshwater dinoflagellate species flock. ISME J. doi:10.1038/ismej.2014.267

Bach, L.T., Riebesell, U., Sett, S., Febiri, S., Rzepka, P., Schulz, K.G., 2012. An approach for particle sinking velocity measurements in the 3–400 µm size range and considerations on the effect of temperature on sinking rates. Mar. Biol. 159, 1853–1864. doi:10.1007/s00227-012-1945-2

Banse, K., 1976. RATES OF GROWTH, RESPIRATION AND PHOTOSYNTHESIS OF UNICELLULAR ALGAE AS RELATED TO CELL SIZE?A REVIEW [2]. J. Phycol. 12, 135–140. doi:10.1111/j.1529-8817.1976.tb00490.x

Coelho, S.M., Simon, N., Ahmed, S., Cock, J.M., Partensky, F., 2013. Ecological and evolutionary genomics of marine photosynthetic organisms. Mol. Ecol. 22, 867–907. doi:10.1111/mec.12000

Ekman, P., Fries, M., 1970. Studies of sediments from Lake Erken, Eastern Central Sweden. Geol. Fören. Stockh. Förh. 92, 214–224. doi:10.1080/11035897009453678

Guillard, R.R.L., Ryther, J.H., 1962. STUDIES OF MARINE PLANKTONIC DIATOMS: I. CYCLOTELLA NANA HUSTEDT, AND DETONULA CONFERVACEA (CLEVE) GRAN. Can. J. Microbiol. 8, 229–239. doi:10.1139/m62-029

Hackett, J.D., Anderson, D.M., Erdner, D.L., Bhattacharya, D., 2004. Dinoflagellates: a remarkable evolutionary experiment. Am. J. Bot. 91, 1523–1534. doi:10.3732/ajb.91.10.1523

Kamykowski, D., Reed, R.E., Kirkpatrick, G.J., 1992. Comparison of sinking velocity, swimming velocity, rotation and path characteristics among six marine dinoflagellate species. Mar. Biol. 113, 319–328.

Kawecki, T.J., Ebert, D., 2004. Conceptual issues in local adaptation. Ecol. Lett. 7, 1225–1241. doi:10.1111/j.1461-0248.2004.00684.x

Klais, R., Tamminen, T., Kremp, A., Spilling, K., Olli, K., 2011. Decadal-Scale Changes of Dinoflagellates and Diatoms in the Anomalous Baltic Sea Spring Bloom. PLoS ONE 6, e21567. doi:10.1371/journal.pone.0021567

Kremp, A., 2001. Effects of cyst resuspension on germination and seeding of two bloom-forming dinoflagellates in the Baltic Sea. Mar. Ecol. Prog. Ser. 216, 57–66. doi:10.3354/meps216057

Kremp, A., 2000. Factors regulating germination of resting cysts of the spring bloom dinoflagellate *Scrippsiella* hangoei from the northern Baltic Sea. J. Plankton Res. 22, 1311–1327.

doi:10.1093/plankt/22.7.1311

Kremp, A., Elbrächter, M., Schweikert, M., Wolny, J.L., Gottschling, M., 2005. WOLOSZYNSKIA HALOPHILA (BIECHELER) COMB. NOV.: A BLOOM-FORMING COLD-WATER DINOFLAGELLATE CO-OCCURRING WITH *SCRIPPSIELLA* HANGOEI (DINOPHYCEAE) IN THE BALTIC SEA1: WOLOSZYNSKIA HALOPHILA (BIECHELER) COMB. NOV. J. Phycol. 41, 629–642. doi:10.1111/j.1529-8817.2005.00070.x

Kuosa, H., 1986. The phytoplankton of a small brackish-water bay, Tvärminne Byviken, southern Finland. Ophelia 4, 119–127.

Larsen, J., Kuosa, H., Ikävalko, J., Kivi, K., Hällfors, S., 1995. A redescription of *Scrippsiella* hangoei (Schiller) comb. nov. –a “red tide” dinoflagellate from the northern Baltic. Phycologia 34, 135–144. doi:10.2216/i0031-8884-34-2-135.1

Laybourn-Parry, J., Pearce, D.A., 2007. The biodiversity and ecology of Antarctic lakes: models for evolution. Philos. Trans. R. Soc. B Biol. Sci. 362, 2273–2289. doi:10.1098/rstb.2006.1945

Lewis, J.M., Marret, F., Bradley, L., 2013. Biological and geological perspectives of dinoflagellates, The Micropalaeontological Society special publications. published for the Micropalaeontological Society by The Geological Society, London.

Lignell, R., Heiskanen, A.S., Kuosa, H., Gundersen, K., Kuuppo-Leinikki, P., Pajuniemi, R., Uitto, A., 1993. Fate of a phytoplankton spring bloom: sedimentation and carbon flow in the planktonic food web in the northern Baltic. Mar. Ecol.-Prog. Ser. 94, 239–239.

Litchman, E., Klausmeier, C.A., 2001. Competition of Phytoplankton under Fluctuating Light. Am. Nat. 157, 170–187. doi:10.1086/318628

Logares, R., Bråte, J., Bertilsson, S., Clasen, J.L., Shalchian-Tabrizi, K., Rengefors, K., 2009. Infrequent marine–freshwater transitions in the microbial world. Trends Microbiol. 17, 414–422. doi:10.1016/j.tim.2009.05.010

Logares, R., Daugbjerg, N., Boltovskoy, A., Kremp, A., Laybourn-Parry, J., Rengefors, K., 2008. Recent evolutionary diversification of a protist lineage. Environ. Microbiol. 10, 1231–1243. doi:10.1111/j.1462-2920.2007.01538.x

Logares, R., Rengefors, K., Kremp, A., Shalchian-Tabrizi, K., Boltovskoy, A., Tengs, T., Shurtleff, A., Klaveness, D., 2007a. Phenotypically Different Microalgal Morphospecies with Identical Ribosomal DNA: A Case of Rapid Adaptive Evolution? Microb. Ecol. 53, 549–561. doi:10.1007/s00248-006-9088-y

Logares, R., Shalchian-Tabrizi, K., Boltovskoy, A., Rengefors, K., 2007b. Extensive dinoflagellate phylogenies indicate infrequent marine–freshwater transitions. Mol. Phylogenet. Evol. 45, 887–903. doi:10.1016/j.ympev.2007.08.005

Malm, J., Bengtsson, L., Terzhevik, A., Boyarinov, P., Glinsky, A., Palshin, N., Petrov, M., 1998. Field

study on currents in a shallow, ice-covered lake. Limnol. Oceanogr. 43, 1669–1679. doi:10.4319/lo.1998.43.7.1669

Mats, V.D., Shcherbakov, D.Y., Efimova, I.M., 2011. Late Cretaceous-Cenozoic history of the Lake Baikal depression and formation of its unique biodiversity. Stratigr. Geol. Correl. 19, 404–423. doi:10.1134/S0869593811040058

Nielsen, S.L., Sand-Jensen, K., 1990. Allometric settling of maximal photosynthetic growth rate to surface/volume ratio. Limnol. Oceanogr. 35, 177–180. doi:10.4319/lo.1990.35.1.0177

Omstedt, A., Axell, L.B., 2003. Modeling the variations of salinity and temperature in the large Gulfs of the Baltic Sea. Cont. Shelf Res. 23, 265–294. doi:10.1016/S0278-4343(02)00207-8

Pettersson, K., 1980. Alkaline phosphatase activity and algal surplus phosphorus as phosphorus-deficiency indicators in Lake Erken. Arch Hydrobiol 89, 54–87.

Rengefors, K., Anderson, D.M., 1998. ENVIRONMENTAL AND ENDOGENOUS REGULATION OF CYST GERMINATION IN TWO FRESHWATER DINOFLAGELLATES. J. Phycol. 34, 568–577. doi:10.1046/j.1529-8817.1998.340568.x

Rengefors, K., Laybourn-Parry, J., Logares, R., Marshall, W.A., Hansen, G., 2008. MARINE-DERIVED DINOFLAGELLATES IN ANTARCTIC SALINE LAKES: COMMUNITY COMPOSITION AND ANNUAL DYNAMICS. J. Phycol. 44, 592–604. doi:10.1111/j.1529-8817.2008.00517.x

Rengefors, K., Legrand, C., 2007. Broad allelopathic activity in *Peridinium aciculiferum* (Dinophyceae). Eur. J. Phycol. 42, 341–349. doi:10.1080/09670260701529604

Rengefors, K., Legrand, C., 2001. Toxicity in *Peridinium aciculiferum* -an adaptive strategy to outcompete other winter phytoplankton? Limnol. Oceanogr. 46, 1990–1997. doi:10.4319/lo.2001.46.8.1990

Rengefors, K., Logares, R., Laybourn-Parry, J., 2012. Polar lakes may act as ecological islands to aquatic protists: LAKES AS ECOLOGICAL ISLANDS TO PROTISTS. Mol. Ecol. 21, 3200–3209. doi:10.1111/j.1365-294X.2012.05596.x

Rengefors, K., Logares, R., Laybourn-Parry, J., Gast, R.J., 2015. Evidence of concurrent local adaptation and high phenotypic plasticity in a polar microeukaryote: Phenotypic plasticity and local adaptation. Environ. Microbiol. 17, 1510–1519. doi:10.1111/1462-2920.12571

Richardson, T.L., Gibson, C.E., Heaney, S.I., 2000. Temperature, growth and seasonal succession of phytoplankton in Lake Baikal, Siberia. Freshw. Biol. 44, 431–440. doi:10.1046/j.1365-2427.2000.00581.x

Shimaraev, M.N., Verbolov, V.I., Granin, N., Sherstayankin, P.P., 1994. Physical limnology of Lake Baikal: a review. BICER, Baikal International Center for Ecological Research.

SMAYDA, T.J., 1970. The suspension and sinking of phytoplankton in the sea.

Suikkanen, S., Hakanen, P., Spilling, K., Kremp, A., 2011. Allelopathic effects of Baltic Sea spring bloom dinoflagellates on co-occurring phytoplankton. Mar. Ecol. Prog. Ser. 439, 45–55. doi:10.3354/meps09356

Sun, J., 2003. Geometric models for calculating cell biovolume and surface area for phytoplankton. J. Plankton Res. 25, 1331–1346. doi:10.1093/plankt/fbg096

Walsby, A.E., Xypolyta, A., 1977. The form resistance of chitan fibres attached to the cells of *Thalassiosira fluviatilis* Hustedt. Br. Phycol. J. 12, 215–223. doi:10.1080/00071617700650231

Wasmund, N., 2003. Phytoplankton trends in the Baltic Sea. ICES J. Mar. Sci. 60, 177–186. doi:10.1016/S1054-3139(02)00280-1

Wasmund, N., Nausch, G., Matthäus, W., 1998. Phytoplankton spring blooms in the southern Baltic Sea—spatio-temporal development and long-term trends. J. Plankton Res. 20, 1099–1117. doi:10.1093/plankt/20.6.1099

Wetzel, R.G., 2001. Limnology: lake and river ecosystems, 3rd ed. ed. Academic Press, San Diego.

Zwartz, D., Bird, M., Stone, J., Lambeck, K., 1998. Holocene sea-level change and ice-sheet history in the Vestfold Hills, East Antarctica. Earth Planet. Sci. Lett. 155, 131–145. doi:10.1016/S0012-821X(97)00204-5

Abstract

The cold-water species *Peridinium aciculiferum* and *Scrippsiella hangoei* form a species flock with small genetic differences but large distinct morphological differences. It has been hypothised that this species flock could be an example of a recent rapid adaptive radition in response to environmental changes such as salinity differences. Here the fine-scale morphology and sinking velocity was studied in the cold-water *Peridinium aciculiferum* / *Scrippsiella hangoei* species flock. Furthermore the freshwater *Peridinium aciculiferum* and the marine-brackish *Scrippsiella hangoei* were competed under constant and fluctuating light conditions. The morphology was analysed in three morphospecies with 8 different populations, including the *Peridinium aciculiferum* morphospecies from Lake Erken and Copenhagen, the *Scrippsiella hangoei* morphospecies from Lake Baikal, Tvärminne, Gulf of Finland and *Scrippsiella* aff. *hangoei* from the Antarctic Lake Abraxas and Lake McNeil and the *Peridinium baicalense* morphospecies from Lake Baikal. For the sinking velocity measurements and the competition experiment 10 strains of each population, the *Peridinium aciculiferum* from Lake Erken and the *Scrippsiella hangoei* from Tvärminne were used and cultured in salinity of 0. The morphology experiment was conducted to measure the morphological differences among and within morphospecies and between freshwater- and marine-brackish species. My objective was to determine weather the freshwater species have obtained a morphology that reduces sinking rate, while the marine-brackish species have retained a spherical shape that increases sinking rate. Further I hypothesised that the species adapted to vertical mixing will dominate under fluctuating light conditions (i. e. turbulent, not ice covered water), while the species adapted to non or horizontal movements will dominate under stable light conditions (stratified, ice covered water). For all cell counts, morphological and sinking velocity measurements the Fluid Imaging Technology (FlowCAM®) was used. My results showed that the marine-brackish species have a more spherical morphology than the freshwater species with a circle fit of 0.87 and 0.77 respectively. The *Peridinium aciculiferum* morphospecies was larger in size and more elongated than the *Scrippsiella hangoei* morphospecies. The sinking velocity results showed a high within-species difference but not among species. There was a strong negative correlation between sinking velocity and surface area to volume ratio and a strong positive correlation between sinking velocity and diameter when tested among strains. In competition *Scrippsiella hangoei* seemed to do slightly better than *Peridinium aciculiferum* when growing both in fluctuating and constant light with mean percentages of 67 % and 55 % respectively. No advantage for *Peridinium aciculiferum* growing under constant light was observed. To conclude, the morphology is not under strong selective pressure in terms of reducing the sinking velocity. This could be explained by the fact that these are swimming species and hence they are able to compensate sinking.

Zusammenfassung

Dinoflagellaten sind allgegenwärtige einzellige Eukaryoten, welche eine wichtige ökologische Rolle in marinen und Süßwasser-Ökosystemen einnehmen (Logares et al., 2008). Sie besitzen eine Vielzahl an Lebensstrategien, als Symbionten, Parasiten, autotroph, heterotroph sowie mixotroph (Hackett et al., 2004). Dinoflagellaten haben eine gewaltige morphologische Diversität und sind wichtige Primärproduzenten in marinen Ökosystemen (Coelho et al., 2013). *Peridinium aciculiferum* bildet in einigen schwedischen Seen die häufigste Art im Winter-Frühlings-Phytoplankton und enorme Blüten unter Eis (Rengefors and Anderson, 1998; Rengefors and Legrand, 2007, 2001), ebenso wie *Scrippsiella hangoei* (Schiller) im nördlichen Teil der Ostsee (Kremp, 2000; Larsen et al., 1995).

Es zeigte sich, dass der Dinoflagellaten-Arten-Flock bestehend aus den marin-brackischen Morphoarten *Scrippsiella hangoei* und *Scrippsiella* aff. *hangoei* und aus den Süßwasser-Morphoarten *Peridinium aciculiferum*, *Peridinium baicalense*, *Peridinium* euryceps und *Scrippsiella hangoei* vom Baikal-See, sehr nah verwandt sind (Annenkova et al., 2015; Logares et al., 2008, 2007a, 2007b; Rengefors et al., 2008). Dieser Arten-Flock mit geringen genetischen Unterschieden ist charakterisiert durch relativ große und deutliche morphologische Unterschieden und durch Unterschiede in der Toleranz von Salinität (Annenkova et al., 2015). Alle Morphoarten kommen nur im Süßwasser vor, außer *S. hangoei*, welche eine breite Salztoleranz (0-30) aufweist und auch in marin-brackischen Ökosystemen vorkommt, wie in der Ostsee und im Polarmeer. Logares et al., 2008 haben angedeutet, dass Unterschiede in Salinität die hauptsächlichen Treiber der Artbildung von *P. aciculiferum* und *S. hangoei* sind. Das erklärt jedoch nicht warum *S. hangoei* im Süßwasser Baikal-See vorkommt, jedoch in den schwedischen Seen nicht (Annenkova et al., 2015). Salinitätsunterschiede aquatischer Lebensräume beeinflussen auch die Dichte des Mediums. Salzwasser hat mit 1.02822 g ml^{-1} bei 4°C eine höhere Dichte als Süßwasser mit 1.0000 g ml^{-1} bei 4°C (Wetzel, 2001) und daher wird vermutet dass der Selektionsdruck auf die Morphologie und die Größe der Zelle um in Schwebe zu bleiben, im Süßwasser größer ist. Daher würden wir annehmen das zwischen den beiden Lebensräumen unterschiedliche Morphotypen vorhanden sind.

In dieser Studie wurde die feinskalige Morphologie und Sinkgeschwindigkeit im Kaltwasser-Arten-Flock *P. aciculiferum* / *S. hangoei* untersucht. Weiters wurde die Süßwasserart *P. aciculiferum* mit der marin-brackischen Art *S. hangoei* unter konstanten und fluktuierenden Lichtbedingungen konkurriert. Die Morphologie wurde insgesamt in drei unterschiedlichen Morphoarten untersucht, wozu 8 verschiedene Populationen ausgewählt wurden und zwar *P. aciculiferum* vom Erken-See und Kopenhagen, *S. hangoei* vom Baikal-See, Golf von Finnland, Tvärminne (Ostsee) und *S.* aff. *hangoei* von den antarktischen Seen Abraxas und McNeil sowie *P. baicalense* vom Baikal-See. Von jeder Population außer von *P. baicalense* wurden 10 unialgale Stämme kultiviert und zur Messung der Morphologie, Wachstumsrate und Zelldichte in regelmäßigen Abständen beprobt. Die Lebendproben wurden ohne Fixierung und sofort nach Beprobung mittels Fluid Imaging Technology (FlowCAM®)

analysiert.

Zur Messung der Sinkgeschwindigkeit und für das Konkurrenz-Experiment wurden 10 unialgale Stämme von *P. aciculiferum* vom Erken-See und *S. hangoei* von Tvärminne ausgewählt und mit Salinität von 0 kultiviert. Die Messungen der Sinkgeschwindigkeit und Zelldichte wurden wiederum mit der FlowCAM® Methode durchgeführt.

Das Morphologie-Experiment wurde durchgeführt, um morphologische Unterschiede zwischen und innerhalb der Morphoarten und zwischen Süßwasser- und marin-brackischen Arten zu messen. Ziel war es, herauszufinden, ob die Süßwasser-Arten eine Morphologie besitzen, welche die Sinkgeschwindigkeit reduziert und ob hingegen die marin-brackischen Arten eine kugelförmige Morphologie aufweisen, welche das Absinken fördert. Weiters wurde angenommen, dass die Art, welche an vertikale Durchmischung angepasst ist, unter fluktuierenden Lichtbedingungen dominieren wird, hingegen unter konstanten Lichtbedingungen jene Art, welche an horizontale Bewegungen angepasst ist, dominieren wird.

Die Ergebnisse haben gezeigt, dass die Morphologie der marin-brackischen Art signifikant kugelförmiger ist als die der Süßwasser-Arten, mit einer dementsprechenden Kreis-Annäherung (circle fit) von 0.87 zu 0.77. Die Morphoart *P. aciculiferum* war signifikant größer und gestreckter als die Morphoart *S. hangoei*. Die Messungen der Sinkgeschwindigkeit zeigten signigikante Unterschiede innerhalb der Art, jedoch nicht zwischen den Arten. Es wurde allerdings eine stark negative Korrelation zwischen Sinkgeschwindigkeit und Oberflächen-Volums-Verhältnis und eine stark positive Korrelation zwischen Sinkgeschwindigkeit und Durchmesser festgestellt. Unter Konkurrenz zeigte *S. hangoei* etwas besseres Wachstum als *P. aciculiferum*, bei beiden Lichtbedingungen. *S. hangoei* erreichte 67 Prozent (unter fluktuierendem Licht) bzw. 55 Prozent (unter konstantem Licht) der gesamten Zellzahl. Das bedeutet, dass *P. aciculiferum* keinen Vorteil bei konstantem Licht besitzt und dass Konkurrenz um Licht als Grund ausgeschlossen werden kann, weswegen *S. hangoei* nicht in schwedischen Seen vorkommt.

Abschließend kann angenommen werden, dass die Dichteunterschiede keinen starken Selektionsdruck auf die Morphologie zur Reduzierung der Sinkgeschwindigkeit, ausüben. Das kann durch die Tatsache erklärt werden, dass dies schwimmende Arten sind und dadurch sind sie in der Lage, das Absinken zu kompensieren.

Curriculum Vitae

Name	**Alina Wiemers**
Nationality	Austria
Date of Birth	13.07.1988
Place of Birth	Oberndorf bei Salzburg, Austria

Education

2010 – 2016	**University of Vienna**
Master Studies	**Ecology and Ecosystems, specialisation in Limnology**
Master Thesis	„Salinity driven speciation through fine-scale morphological adaptations in the dinoflagellate species flock *Peridinium aciculiferum*/*Scrippsiella hangoei*“
Supervision	Karin Rengefors, Aquatic Ecology Unit – Department of Biology Lund University
Mentor	Michael Schagerl, Phycology Unit – Department of Limnology & Bio-Oceanography, University of Vienna
Targeted Degree	Master of Science
2014 – 2015	**Lund University**
Programme	**Erasmus-Exchange year in Lund, Sweden** Laboratory work for master thesis, Algae Lab, Aquatic Ecology Unit Field course in Limnology
2013 –	**University of Vienna**
Master Studies	**Conservation Biology and Biodiversity Management**
07/2013	**WasserCluster Lunz**
Programme	**Working group AQUASCALE, FEMtech funding** Laboratory and limnological field work
2008 – 2012	**University of Vienna**
Bachelor Studies	**Biology, specialisation in Ecology**
Bachelor Thesis	“Snapshot of algal communities at selected ponds and lakes in and around the Neusiedler See region, Burgenland”
Degree	Bachelor of Science
2002 – 2007	**Secondary School for Economic Professions** HBLA Neumarkt am Wallersee
Degree	Matura
1998 – 2002	**Secondary Modern School Köstendorf**
1994 – 1998	**Elementary School Köstendorf**

Appendix

Exp. 1. Intra- and interspecific variations in morphology (Hypothesis 1)

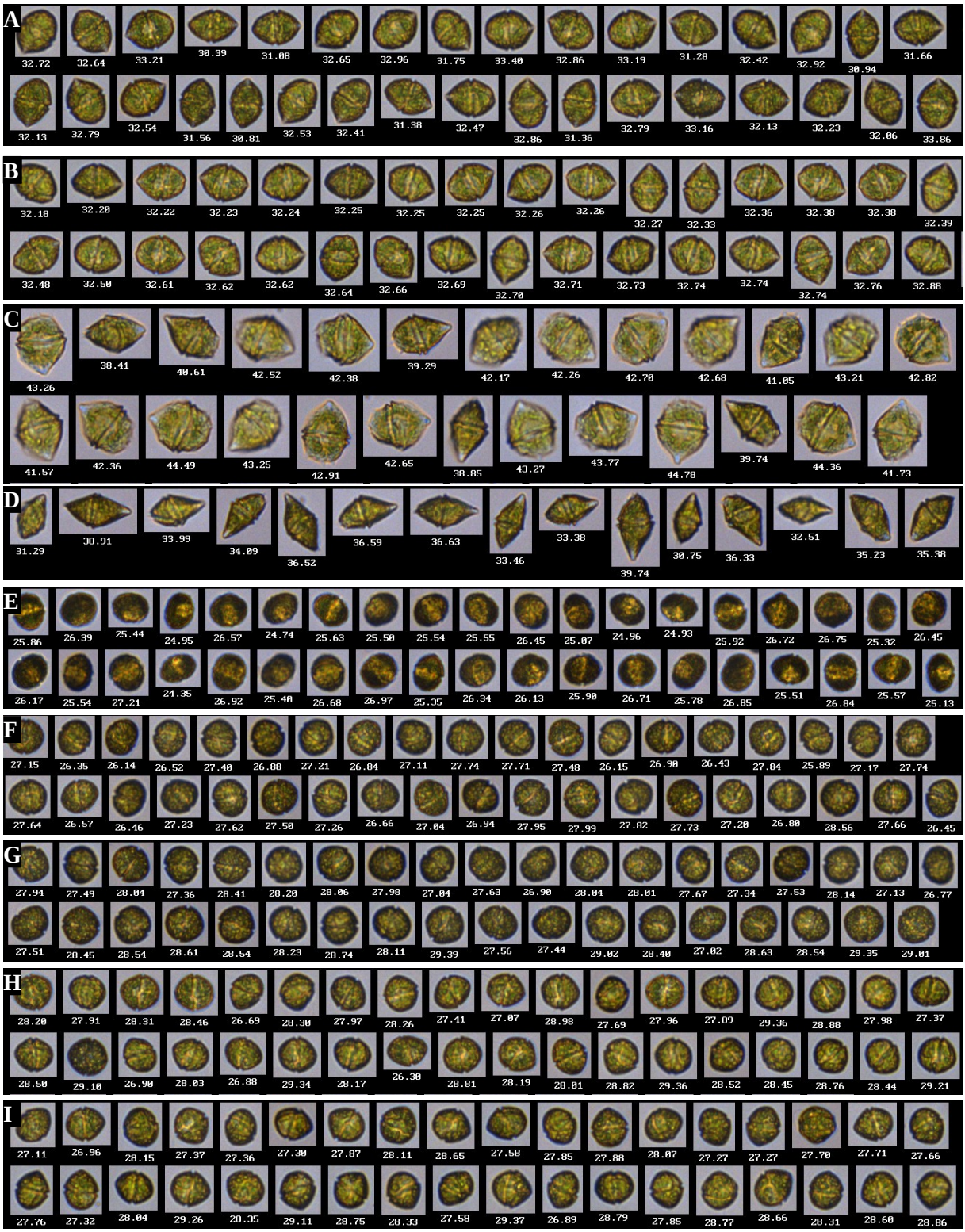

Figure. 10: FlowCAM pictures of all populations, measured with Trigger Mode (FC100, 10x objective), cells from the upper size range were selected, pictured from the ventral or dorsal side except D (left or right side), numbers are given as diameter ESD (µm), **(A)** *P. aciculiferum* Copenhagen (Cop), **(B)** *P. aciculiferum* L. Erken, **(C-D)** *P. baicalense* L. Baikal, **(E)** *S. hangoei* L. Baikal, **(F)** *S. hangoei* L. Abraxas, **(G)** *S. hangeoi* L. McNeil, **(H)** *S. hangoei* Gulf of Finland, **(I)** *S. hangoei* Tvärminne Baltic Sea

Table 8: Overview of mean growth rate d^{-1}, divisions d^{-1} and doubling time per strain

Strains	Populations	Morphospecies	Mean growth rate day^{-1}	Divisions day^{-1}	Doubling time
Abra127	Abra	SH	0.127	0.183	5.5
Abra132	Abra	SH	0.098	0.141	7.1
Abra134	Abra	SH	0.102	0.147	6.8
Abra135	Abra	SH	0.204	0.294	3.4
Abra136	Abra	SH	0.081	0.116	8.6
Abra181	Abra	SH	0.166	0.240	4.2
Abra44	Abra	SH	0.106	0.152	6.6
AbraT35	Abra	SH	0.120	0.173	5.8
AbraT39	Abra	SH	0.113	0.163	6.1
AbraT40	Abra	SH	0.130	0.188	5.3
Cop1	Cop	PA	0.103	0.149	6.7
Cop10	Cop	PA	0.153	0.221	4.5
Cop13	Cop	PA	0.135	0.194	5.1
Cop14	Cop	PA	0.147	0.212	4.7
Cop2	Cop	PA	0.096	0.139	7.2
Cop3	Cop	PA	0.131	0.189	5.3
Cop6	Cop	PA	0.177	0.256	3.9
Cop7	Cop	PA	0.078	0.113	8.9
Cop8	Cop	PA	0.179	0.258	3.9
Cop9	Cop	PA	0.122	0.176	5.7
Erk1	Erk	PA	0.217	0.313	3.2
Erk16B	Erk	PA	0.114	0.164	6.1
Erk1B	Erk	PA	0.172	0.248	4.0
Erk2	Erk	PA	0.249	0.360	2.8
Erk2B	Erk	PA	0.122	0.175	5.7
Erk3B	Erk	PA	0.146	0.210	4.8
Erk4	Erk	PA	0.124	0.179	5.6
Erk5	Erk	PA	0.110	0.158	6.3
Erk6	Erk	PA	0.141	0.204	4.9
Erk8	Erk	PA	0.138	0.199	5.0
McNeil109	McNeil	SH	0.136	0.197	5.1
McNeil161	McNeil	SH	0.111	0.160	6.2
McNeil190	McNeil	SH	0.117	0.169	5.9
McNeil205	McNeil	SH	0.079	0.114	8.8
McNeil207	McNeil	SH	0.149	0.215	4.7
McNeil208	McNeil	SH	0.101	0.145	6.9
McNeil209	McNeil	SH	0.140	0.201	5.0
McNeil210	McNeil	SH	0.114	0.165	6.1
McNeil221	McNeil	SH	0.105	0.152	6.6
McNeilT7	McNeil	SH	0.130	0.187	5.3
PB2-202	PB2	PB	0.201	0.289	4.1
SHLL7-1301	SHLL7	SH	0.166	0.239	4.2
SHLL7-1303	SHLL7	SH	0.188	0.272	3.7
SHLL7-1304	SHLL7	SH	0.188	0.272	3.7
SHLL7-1305	SHLL7	SH	0.193	0.278	3.6
SHLL7-1306	SHLL7	SH	0.161	0.232	4.3
SHLL7-1308	SHLL7	SH	0.257	0.371	2.7
SHLL7-1310	SHLL7	SH	0.153	0.221	4.5
SHLL7-1311	SHLL7	SH	0.161	0.232	4.3
SHLL7-1318	SHLL7	SH	0.201	0.290	3.4
SHLL7-1321	SHLL7	SH	0.156	0.226	4.4
SHTV906	SHTV	SH	0.178	0.256	3.9
SHTV908	SHTV	SH	0.128	0.184	5.4
SHTV909	SHTV	SH	0.169	0.243	4.1
SHTV912	SHTV	SH	0.170	0.245	4.1
SHTV913	SHTV	SH	0.172	0.248	4.0
SHTV914	SHTV	SH	0.136	0.196	5.1
SHTV916	SHTV	SH	0.113	0.163	6.1
SHTV918	SHTV	SH	0.151	0.218	4.6
SHTV919	SHTV	SH	0.178	0.257	3.9
SHTV922	SHTV	SH	0.193	0.278	3.6

Table 9a: Overview of selected particle properties per strain (Diameter ESD, Length and Width as µm)

Strains	Populations	Morphospecies	Aspect Ratio	Circle Fit	Convexity	Diameter ESD (µm)	Length (µm)	Width (µm)	Symmetry
Abra127	Abra	SH	0.91	0.90	1.00	24.58	26.07	23.19	0.92
Abra132	Abra	SH	0.91	0.89	1.00	24.80	26.40	23.28	0.92
Abra134	Abra	SH	0.90	0.89	1.00	25.99	27.60	24.47	0.92
Abra135	Abra	SH	0.91	0.90	1.00	25.66	27.15	24.26	0.92
Abra136	Abra	SH	0.91	0.90	1.00	25.62	27.17	24.13	0.92
Abra181	Abra	SH	0.89	0.88	1.00	25.51	27.30	23.82	0.92
Abra44	Abra	SH	0.89	0.88	1.00	26.40	28.35	24.63	0.91
AbraT35	Abra	SH	0.92	0.90	1.00	25.00	26.45	23.65	0.92
AbraT39	Abra	SH	0.92	0.91	1.00	24.96	26.24	23.58	0.92
AbraT40	Abra	SH	0.91	0.90	1.00	24.85	26.30	23.43	0.92
Cop10	Cop	PA	0.76	0.74	1.00	28.26	33.46	24.38	0.90
Cop13	Cop	PA	0.76	0.75	1.00	26.05	30.85	22.49	0.90
Cop14	Cop	PA	0.76	0.75	1.00	28.58	33.76	24.71	0.90
Cop1	Cop	PA	0.75	0.74	1.00	26.79	31.66	23.01	0.90
Cop2	Cop	PA	0.77	0.76	1.00	28.97	34.09	25.24	0.90
Cop3	Cop	PA	0.77	0.75	1.00	29.13	34.40	25.28	0.90
Cop6	Cop	PA	0.73	0.72	1.00	27.04	32.48	22.92	0.90
Cop7	Cop	PA	0.75	0.73	1.00	27.95	33.20	23.87	0.90
Cop8	Cop	PA	0.74	0.73	1.00	27.41	32.72	23.32	0.90
Cop9	Cop	PA	0.77	0.76	1.00	28.65	33.60	24.93	0.90
Erk16B	Erk	PA	0.75	0.74	1.00	26.83	31.71	23.09	0.89
Erk1B	Erk	PA	0.75	0.72	0.97	29.06	33.91	24.82	0.85
Erk1	Erk	PA	0.78	0.75	0.98	28.77	33.04	25.11	0.85
Erk2B	Erk	PA	0.79	0.77	1.00	29.14	33.85	25.73	0.91
Erk2	Erk	PA	0.77	0.74	0.97	28.12	32.48	24.26	0.84
Erk3B	Erk	PA	0.75	0.72	0.98	28.52	33.37	24.40	0.85
Erk4	Erk	PA	0.77	0.76	1.00	28.34	33.15	24.77	0.91
Erk5	Erk	PA	0.77	0.75	1.00	27.76	32.65	24.08	0.90
Erk6	Erk	PA	0.73	0.71	1.00	27.06	32.78	22.83	0.89
Erk8	Erk	PA	0.77	0.74	0.97	29.75	34.08	25.84	0.84
McNeil109	McNeil	SH	0.89	0.88	1.00	26.06	27.77	24.31	0.91
McNeil161	McNeil	SH	0.90	0.89	1.00	26.20	27.81	24.54	0.91
McNeil190	McNeil	SH	0.93	0.86	0.96	28.25	29.69	26.66	0.85
McNeil205	McNeil	SH	0.92	0.91	1.00	24.88	26.21	23.48	0.92
McNeil207	McNeil	SH	0.91	0.90	1.00	25.76	27.24	24.19	0.91
McNeil208	McNeil	SH	0.91	0.87	0.98	26.90	28.48	25.24	0.85
McNeil209	McNeil	SH	0.92	0.91	1.00	23.09	24.29	21.83	0.91
McNeil210	McNeil	SH	0.91	0.90	1.00	25.43	26.84	23.95	0.91
McNeil221	McNeil	SH	0.90	0.89	1.00	25.54	27.10	23.92	0.91
McNeilT7	McNeil	SH	0.90	0.86	0.98	26.54	28.28	24.72	0.86
PB2-202	PB2	PB	0.79	0.72	0.97	37.99	43.49	33.17	0.80
SHB02	SHB	SH	0.81	0.82	1.00	22.54	25.03	19.75	0.91
SHB07	SHB	SH	0.81	0.82	1.00	21.62	24.03	18.94	0.90
SHB08	SHB	SH	0.81	0.82	1.00	23.01	25.53	20.26	0.91
SHB09	SHB	SH	0.84	0.84	1.00	21.77	23.86	19.39	0.91
SHB11	SHB	SH	0.83	0.83	1.00	22.31	24.54	19.78	0.91
SHB12	SHB	SH	0.86	0.86	1.00	21.37	23.14	19.23	0.92
SHB14	SHB	SH	0.83	0.84	1.00	19.94	21.88	17.71	0.90
SHB15	SHB	SH	0.82	0.82	1.00	22.09	24.44	19.45	0.90
SHB16	SHB	SH	0.82	0.82	1.00	23.79	26.23	21.04	0.91
SHB17	SHB	SH	0.81	0.81	1.00	23.71	26.32	20.78	0.91
SHLL7-1301	SHLL7	SH	0.87	0.87	1.00	22.95	24.77	21.22	0.91
SHLL7-1303	SHLL7	SH	0.85	0.85	1.00	22.72	24.96	20.79	0.91
SHLL7-1304	SHLL7	SH	0.89	0.88	1.00	24.08	25.93	22.40	0.92
SHLL7-1305	SHLL7	SH	0.87	0.84	0.99	22.60	24.66	20.66	0.86
SHLL7-1306	SHLL7	SH	0.87	0.84	0.99	24.51	26.74	22.40	0.87
SHLL7-1308	SHLL7	SH	0.87	0.85	0.99	22.91	24.80	21.02	0.87
SHLL7-1310	SHLL7	SH	0.88	0.85	0.98	23.64	25.60	21.72	0.85
SHLL7-1311	SHLL7	SH	0.88	0.86	0.99	23.55	25.36	21.74	0.87
SHLL7-1318	SHLL7	SH	0.85	0.85	1.00	24.11	26.40	22.05	0.92
SHLL7-1321	SHLL7	SH	0.89	0.85	0.98	26.95	29.21	24.88	0.86
SHTV906	SHTV	SH	0.84	0.82	0.99	25.06	27.78	22.68	0.86
SHTV908	SHTV	SH	0.83	0.82	1.00	26.51	29.60	23.93	0.92
SHTV909	SHTV	SH	0.88	0.85	0.98	25.18	27.28	23.19	0.86
SHTV912	SHTV	SH	0.85	0.84	1.00	24.61	27.21	22.42	0.90
SHTV913	SHTV	SH	0.84	0.83	0.99	23.74	26.27	21.47	0.87
SHTV914	SHTV	SH	0.85	0.82	0.98	28.03	31.02	25.42	0.86
SHTV916	SHTV	SH	0.83	0.82	1.00	24.83	27.88	22.34	0.91
SHTV918	SHTV	SH	0.83	0.81	0.99	26.69	29.57	23.96	0.87
SHTV919	SHTV	SH	0.86	0.82	0.99	26.08	28.81	23.73	0.86
SHTV922	SHTV	SH	0.86	0.84	0.99	24.78	27.19	22.56	0.87

Table 9b: Overview of selected particle properties per strain

Strains	Pop-ulations	Morpho-species	Surface Area (µm²)	Volume (µm³)	SA:V calculated	Area Filled (µm²)	Volume ESD (µm³)	SA:V FlowCAM
Abra127	Abra	SH	1842.0	7471.2	0.25	455.9	7910.5	0.06
Abra132	Abra	SH	1867.0	7617.2	0.25	463.5	8124.8	0.06
Abra134	Abra	SH	2055.2	8801.3	0.24	510.5	9350.1	0.06
Abra135	Abra	SH	2010.5	8533.3	0.24	498.5	9025.3	0.06
Abra136	Abra	SH	1997.6	8441.3	0.24	496.7	8967.5	0.06
Abra181	Abra	SH	1969.9	8250.5	0.24	491.2	8848.5	0.06
Abra44	Abra	SH	2112.7	9158.9	0.24	524.6	9791.9	0.05
AbraT35	Abra	SH	1909.1	7888.7	0.25	472.6	8338.4	0.06
AbraT39	Abra	SH	1894.0	7816.2	0.25	471.8	8330.0	0.06
AbraT40	Abra	SH	1876.1	7666.6	0.25	465.8	8146.8	0.06
Cop10	Cop	PA	2113.9	8786.5	0.25	576.9	12046.1	0.05
Cop13	Cop	PA	1810.6	6930.9	0.26	488.9	9283.6	0.05
Cop14	Cop	PA	2163.5	9056.0	0.24	590.3	12308.3	0.05
Cop1	Cop	PA	1916.8	7573.5	0.26	518.3	10120.3	0.05
Cop2	Cop	PA	2255.4	9732.2	0.24	610.1	12978.3	0.05
Cop3	Cop	PA	2263.9	9720.8	0.24	612.8	13078.3	0.05
Cop6	Cop	PA	1908.1	7432.2	0.26	521.6	10408.2	0.05
Cop7	Cop	PA	2044.7	8277.2	0.25	561.7	11468.8	0.05
Cop8	Cop	PA	1962.2	7786.1	0.26	539.2	10896.6	0.05
Cop9	Cop	PA	2179.7	9229.9	0.24	598.2	12556.7	0.05
Erk16B	Erk	PA	1948.5	7832.1	0.25	520.4	10307.3	0.05
Erk1B	Erk	PA	2184.6	9221.5	0.24	579.4	13048.3	0.05
Erk1	Erk	PA	2192.9	9385.6	0.24	578.3	12732.1	0.05
Erk2B	Erk	PA	2299.5	10067.7	0.23	623.3	13202.1	0.05
Erk2	Erk	PA	2072.7	8585.3	0.25	546.1	11849.7	0.05
Erk3B	Erk	PA	2123.8	8832.9	0.24	560.4	12272.9	0.05
Erk4	Erk	PA	2149.4	9055.5	0.24	588.3	12129.2	0.05
Erk5	Erk	PA	2067.1	8545.0	0.25	560.4	11427.2	0.05
Erk6	Erk	PA	1925.6	7529.8	0.26	516.8	10422.3	0.05
Erk8	Erk	PA	2356.3	10470.9	0.23	614.5	14022.9	0.05
McNeil109	McNeil	SH	2048.8	8762.1	0.24	513.8	9441.1	0.06
McNeil161	McNeil	SH	2075.5	8942.1	0.24	519.7	9591.3	0.06
McNeil190	McNeil	SH	2409.3	11123.4	0.22	561.8	11885.6	0.05
McNeil205	McNeil	SH	1879.6	7712.7	0.25	468.2	8218.8	0.06
McNeil207	McNeil	SH	2005.7	8487.2	0.24	502.2	9102.7	0.06
McNeil208	McNeil	SH	2183.7	9617.0	0.23	519.8	10322.1	0.05
McNeil209	McNeil	SH	1621.6	6182.2	0.27	402.5	6571.5	0.06
McNeil210	McNeil	SH	1960.1	8202.7	0.24	490.0	8759.1	0.06
McNeil221	McNeil	SH	1970.7	8263.2	0.24	492.9	8862.2	0.06
McNeilT7	McNeil	SH	2120.8	9234.3	0.24	508.8	9977.0	0.05
PB2-202	PB2	PB	3554.5	18889.0	0.19	999.5	29535.9	0.04
SHB02	SHB	SH	1452.9	5155.3	0.29	374.8	6047.0	0.06
SHB07	SHB	SH	1338.5	4560.8	0.30	344.3	5344.1	0.07
SHB08	SHB	SH	1529.0	5604.3	0.28	393.3	6511.8	0.06
SHB09	SHB	SH	1385.2	4893.4	0.30	354.4	5618.6	0.07
SHB11	SHB	SH	1445.0	5178.5	0.29	370.5	5973.8	0.06
SHB12	SHB	SH	1336.1	4623.5	0.30	342.4	5262.6	0.07
SHB14	SHB	SH	1161.3	3765.7	0.32	296.8	4338.7	0.07
SHB15	SHB	SH	1412.4	5006.8	0.29	362.8	5832.5	0.06
SHB16	SHB	SH	1640.2	6254.1	0.27	421.6	7230.7	0.06
SHB17	SHB	SH	1618.2	6119.1	0.27	418.3	7168.9	0.06
SHLL7-1301	SHLL7	SH	1582.9	5930.2	0.27	394.3	6423.8	0.06
SHLL7-1303	SHLL7	SH	1547.8	5707.2	0.28	384.3	6203.9	0.06
SHLL7-1304	SHLL7	SH	1754.1	6930.9	0.26	436.2	7439.2	0.06
SHLL7-1305	SHLL7	SH	1519.7	5538.6	0.28	364.8	6076.3	0.06
SHLL7-1306	SHLL7	SH	1788.3	7077.2	0.26	430.7	7767.4	0.06
SHLL7-1308	SHLL7	SH	1559.9	5765.5	0.27	378.3	6323.9	0.06
SHLL7-1310	SHLL7	SH	1665.7	6368.0	0.26	394.7	6965.7	0.06
SHLL7-1311	SHLL7	SH	1654.7	6304.7	0.26	397.9	6869.3	0.06
SHLL7-1318	SHLL7	SH	1743.9	6862.8	0.26	435.9	7499.3	0.06
SHLL7-1321	SHLL7	SH	2177.8	9512.9	0.23	515.3	10294.9	0.05
SHTV906	SHTV	SH	1870.2	7568.6	0.25	451.5	8332.4	0.06
SHTV908	SHTV	SH	2100.0	9013.4	0.24	524.9	9900.8	0.05
SHTV909	SHTV	SH	1907.2	7877.4	0.25	453.7	8572.1	0.05
SHTV912	SHTV	SH	1817.2	7267.0	0.25	451.9	7919.6	0.06
SHTV913	SHTV	SH	1676.1	6427.5	0.27	406.9	7094.3	0.06
SHTV914	SHTV	SH	2349.9	10714.4	0.22	563.0	11767.6	0.05
SHTV916	SHTV	SH	1839.7	7368.0	0.25	457.4	8108.2	0.06
SHTV918	SHTV	SH	2105.3	9068.2	0.24	514.0	10155.7	0.05
SHTV919	SHTV	SH	2031.4	8557.2	0.24	485.1	9357.8	0.05
SHTV922	SHTV	SH	1833.6	7386.5	0.25	444.6	8126.6	0.06

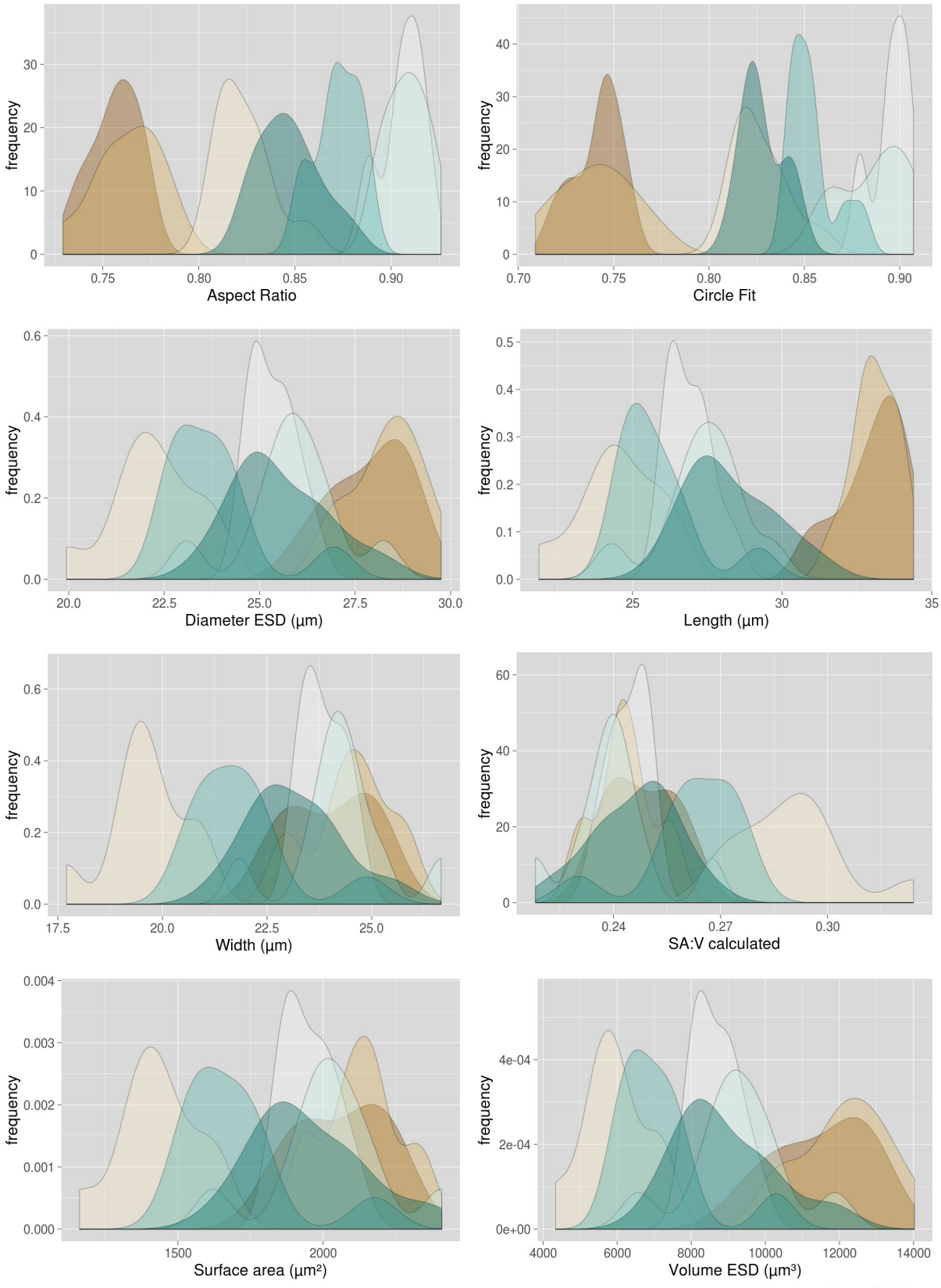

Figure. 12: Frequency plots of selected particle properties including all populations except *P. baicalense* (PB)

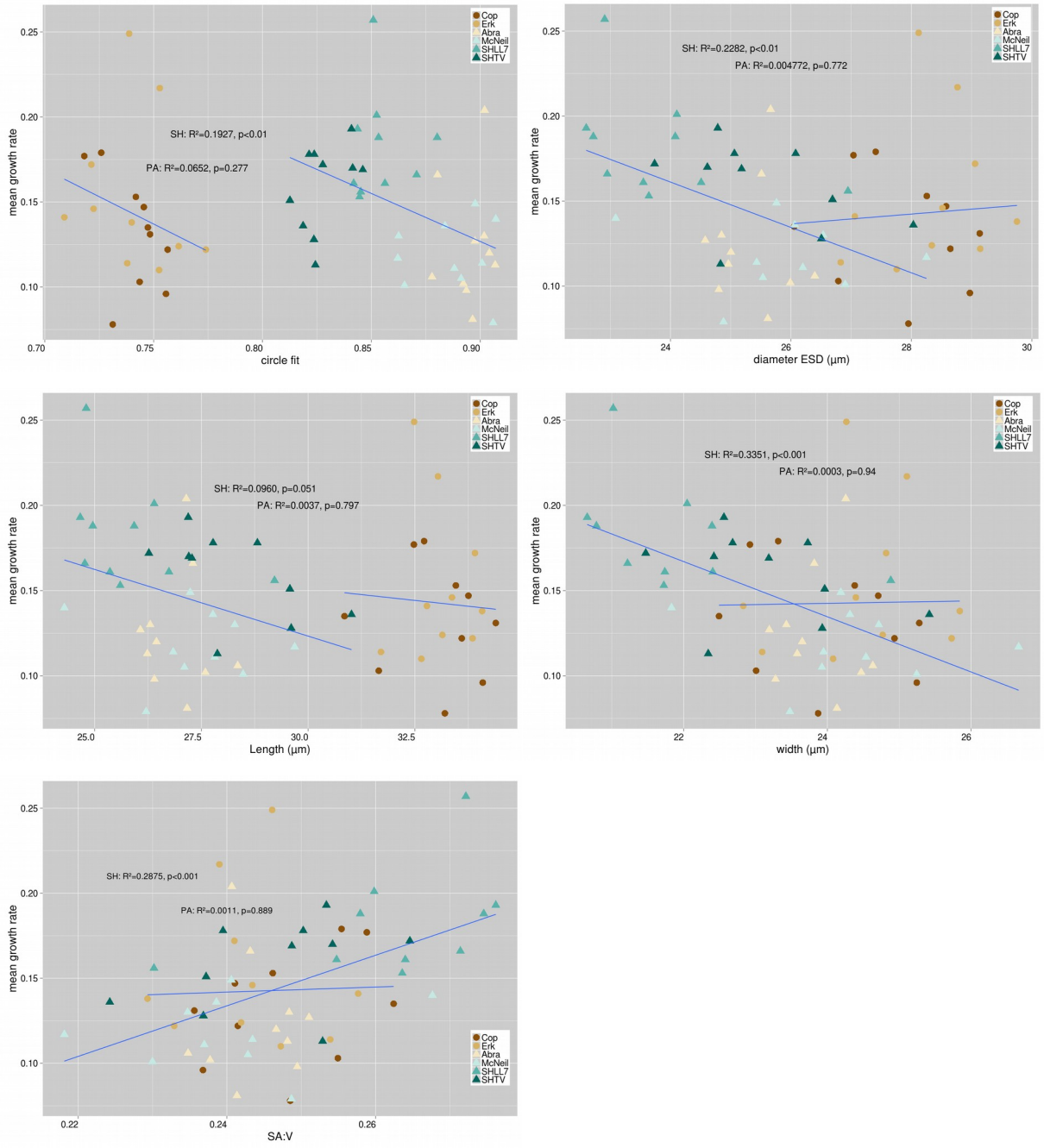

Figure. 13: Linear regression between mean growth rate and different size properties for all populations excluding *P. baicalense*, regression lines plotted for each morphospecies, PA and circles stands for the *P. aciculiferum* morphospecies, SH and triangles stands for the *S. hangoei* morphospecies

Exp. 2. Sinking rates (Hypothesis 1)

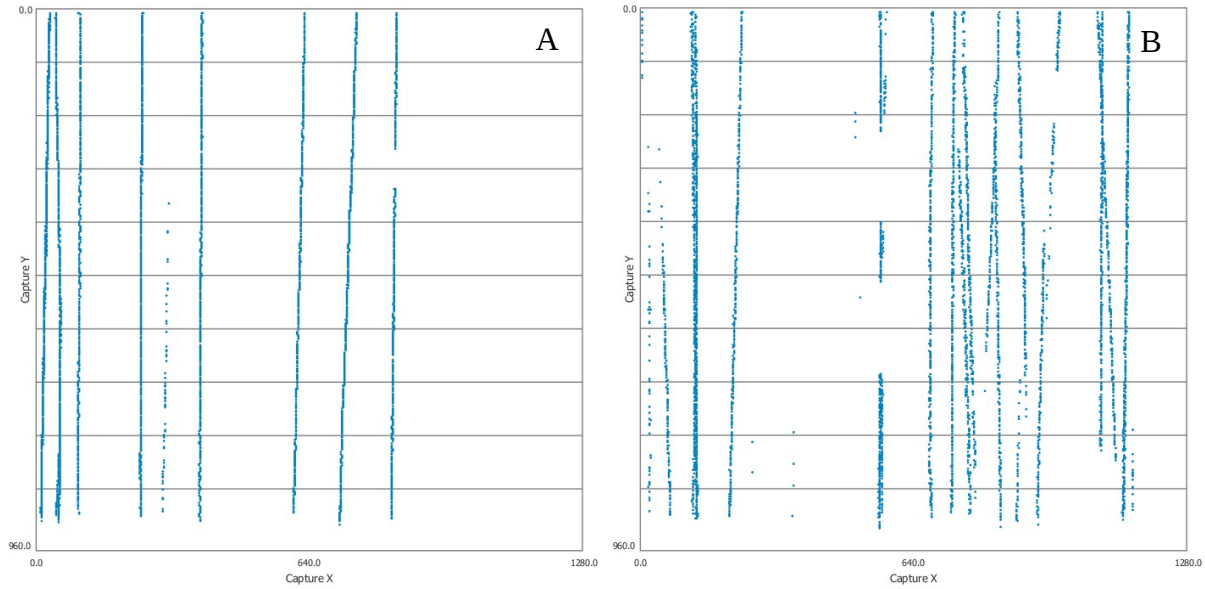

Figure. 14: X- and Y-position (pixels) of selected cells (focused) for sinking rate analysis, when sinking through the FlowCAM glass cuvette and photographed by the camera during the measurement. Each dotted line represents a trajectory of an individual cell. **A** - *P. aciculiferum* of Lake Erken (strain Erk5), **B** – *S. hangeoi* from Tvärminne (strain SHTV909).

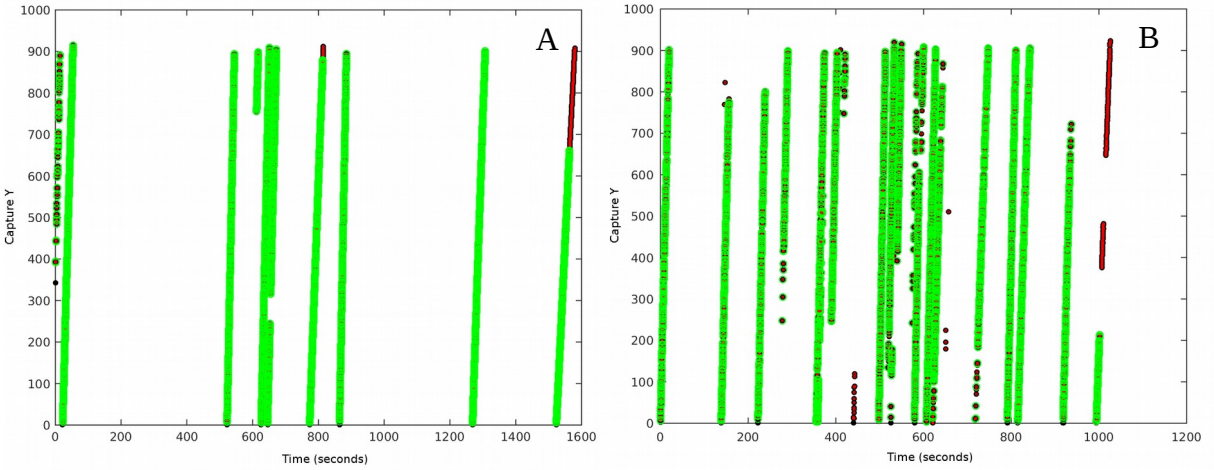

Figure. 15: Y-position of selected cells (focused) on the display window plotted against the exact time the cells were photographed. **A** - *P. aciculiferum* of Lake Erken (strain Erk5), **B** – *S. hangeoi* from Tvärminne (strain SHTV909). The slopes of each trajectory (dotted lines) represent individual sinking velocities. The faster a particle is sinking, the steeper the slope. Green circles mark those cells which were analysed and used to calculate the sinking velocities by the MATLAB script with a fit of $R^2 \geq 0.95$. (Bach et al., 2012)

Table 10: Overview of sinking velocity calculations and measured particle properties per strain

Strain	Pop-ulation	Morpho-species	Sinking Velocity m d^{-1}	SA:V calculated	Volume (µm³)	Surface Area (µm²)	Circle Fit	Diameter ESD (µm)	Length (µm)	Width (µm)
Erk1	Erk	PA	2.21 (0.41)	0.23 (0.02)	10729.8 (2304.8)	2403.0 (337.5)	0.75 (0.04)	30.4 (1.9)	34.6 (2.4)	26.3 (2.1)
Erk1B	Erk	PA	1.08 (0.42)	0.28 (0.03)	6273.3 (2091.9)	1685.1 (378.6)	0.73 (0.07)	25.7 (2.9)	30.1 (4.0)	21.5 (2.2)
Erk2	Erk	PA	1.42 (0.37)	0.26 (0.03)	7204.5 (2465.7)	1830.1 (420.1)	0.75 (0.06)	26.6 (2.9)	30.2 (3.5)	22.8 (2.9)
Erk2B	Erk	PA	2.20 (0.33)	0.21 (0.01)	12604.5 (1180.4)	2680.3 (170.6)	0.74 (0.03)	31.6 (0.9)	36.2 (1.6)	28.1 (0.9)
Erk3B	Erk	PA	1.25 (0.27)	0.28 (0.02)	5682.3 (1447.4)	1566.1 (267.5)	0.82 (0.08)	24.4 (2.2)	27.3 (3.5)	21.6 (1.5)
Erk4	Erk	PA	1.79 (0.18)	0.24 (0.02)	9072.9 (2150.9)	2139.5 (354.8)	0.78 (0.05)	28.4 (2.4)	31.9 (3.8)	25.3 (1.9)
Erk5	Erk	PA	1.52 (0.50)	0.26 (0.02)	7369.2 (1969.8)	1868.8 (334.2)	0.75 (0.06)	27.0 (2.4)	30.8 (3.0)	23.0 (2.2)
Erk6	Erk	PA	2.58 (0.18)	0.22 (0.03)	13056.0 (2296.6)	2780.8 (385.1)	0.66 (0.10)	32.7 (2.7)	39.6 (4.9)	27.3 (2.0)
Erk7	Erk	PA	2.00 (0.34)	0.23 (0.01)	9767.7 (1485.1)	2251.0 (217.1)	0.75 (0.03)	28.9 (1.1)	32.9 (1.3)	25.5 (1.4)
PB2-202	PB2	PB	1.81 (0.40)	0.23 (0.03)	12339.9 (5677.7)	2649.2 (778.9)	0.64 (0.10)	32.9 (4.8)	38.1 (4.4)	27.4 (5.7)
SHTV1006	SHTV	SH	1.16 (0.17)	0.28 (0.02)	5253.8 (1338.5)	1467.9 (245.5)	0.82 (0.07)	22.7 (1.9)	25.2 (2.7)	19.8 (1.7)
SHTV1008	SHTV	SH	1.25 (0.14)	0.28 (0.02)	5357.3 (1083.1)	1487.8 (198.2)	0.83 (0.05)	22.8 (1.5)	25.1 (1.9)	20.1 (1.4)
SHTV901	SHTV	SH	1.45 (0.32)	0.26 (0.02)	6610.8 (1301.6)	1707.4 (226.7)	0.85 (0.04)	24.4 (1.7)	26.4 (2.0)	21.8 (1.5)
SHTV908	SHTV	SH	2.08 (0.69)	0.23 (0.02)	10529.0 (3608.5)	2312.4 (497.1)	0.84 (0.05)	28.1 (2.8)	30.4 (3.6)	25.3 (2.5)
SHTV909	SHTV	SH	2.27 (0.41)	0.24 (0.02)	8549.4 (2234.2)	2019.2 (347.2)	0.83 (0.04)	26.3 (2.1)	28.4 (2.2)	23.7 (2.3)
SHTV913	SHTV	SH	2.31 (0.43)	0.22 (0.02)	11782.8 (2573.7)	2509.1 (365.5)	0.82 (0.04)	29.6 (2.1)	32.2 (2.2)	26.2 (2.1)
SHTV914	SHTV	SH	1.36 (0.21)	0.26 (0.02)	6603.2 (1457.0)	1705.5 (252.3)	0.85 (0.05)	24.3 (2.0)	26.4 (2.7)	21.7 (1.4)
SHTV916	SHTV	SH	1.75 (0.23)	0.24 (0.01)	8848.0 (1534.0)	2082.4 (236.0)	0.79 (0.03)	27.3 (1.5)	30.0 (1.6)	23.6 (1.5)
SHTV919	SHTV	SH	1.60 (0.27)	0.24 (0.02)	8509.2 (2791.6)	2011.2 (413.2)	0.82 (0.04)	26.4 (2.3)	28.9 (2.5)	23.4 (2.6)
SHTV921	SHTV	SH	1.31 (0.28)	0.28 (0.03)	5636.1 (1822.2)	1528.4 (322.9)	0.84 (0.04)	23.0 (2.3)	25.3 (2.9)	20.3 (2.1)

Table 11: Overview of mean growth rate d^{-1}, divisions d^{-1} and doubling time per sinking rate strain, grown under salinity of 0.

Strains	Populations	Morphospecies	Mean growth rate day^{-1}	Divisions day^{-1}	Doubling time
Erk1	Erk	PA	0.120	0.172	5.8
Erk1B	Erk	PA	0.068	0.098	10.2
Erk2	Erk	PA	0.094	0.135	7.4
Erk2B	Erk	PA	0.149	0.215	4.7
Erk3B	Erk	PA	0.109	0.157	6.4
Erk4	Erk	PA	0.155	0.223	4.5
Erk5	Erk	PA	0.077	0.111	9.0
Erk6	Erk	PA	0.185	0.267	3.7
Erk7	Erk	PA	0.119	0.172	5.8
PB2-202	PB2	PB	0.200	0.289	4.1
SHTV1006	SHTV	SH	0.078	0.112	8.9
SHTV1008	SHTV	SH	0.133	0.191	5.2
SHTV901	SHTV	SH	0.167	0.240	4.2
SHTV908	SHTV	SH	0.461	0.665	1.5
SHTV909	SHTV	SH	0.222	0.321	3.1
SHTV913	SHTV	SH	0.102	0.148	6.8
SHTV914	SHTV	SH	0.075	0.108	9.2
SHTV916	SHTV	SH	0.090	0.129	7.7
SHTV919	SHTV	SH	0.084	0.121	8.3
SHTV921	SHTV	SH	0.104	0.151	6.6

Table 12: Overview calculation outcomes of the narcotisation experiment for each strain and replicate

Strains	Replicates	Cells ml^{-1}	Vi sample (µl)	Nicotine / Ethanol (µl)	Vi SYTOX (µl)	Vf (µl)	Mi SYTOX (µM)	Mf SYTOX (µM)
Erk6	1	21600	1000	25	2	1027	30	0.058
SHTV908	1	25560	1000	25	2	1027	30	0.058
Abra134	1	18720	1000	25	2	1027	30	0.058
PB2-202	1	34056	1000	25	2	1027	30	0.058
Erk6	2	21600	1000	50	2	1052	30	0.057
SHTV908	2	25560	1000	50	2	1052	30	0.057
Abra134	2	18720	1000	50	2	1052	30	0.057
PB2-202	2	34056	1000	50	2	1052	30	0.057
Erk6	3	21600	1000	100	2	1102	30	0.054
SHTV908	3	25560	1000	100	2	1102	30	0.054
Abra134	3	18720	1000	100	2	1102	30	0.054
PB2-202	3	34056	1000	100	2	1102	30	0.054
Erk6	dead cell control	21600	1000	150	2	1152	30	0.052
SHTV908	dead cell control	25560	1000	150	2	1152	30	0.052
Abra134	dead cell control	18720	1000	150	2	1152	30	0.052
PB2-202	dead cell control	34056	1000	150	2	1152	30	0.052
Erk6	live cell control	21600	1000	0	2	1002	30	0.060
SHTV908	live cell control	25560	1000	0	2	1002	30	0.060
Abra134	live cell control	18720	1000	0	2	1002	30	0.060
PB2-202	live cell control	34056	1000	0	2	1002	30	0.060

Exp. 3. Competition experiment (Hypothesis 2)

Figure. 16: Extrapolation outcomes for the constant and fluctuating light, per replicate and day of the competition cultures *S. hangoei* from Tvärminne (SHTV in red) and *P. aciculiferum* from L Erken (Erk in blue). Y-axis: extrapolated mean percentages of the total number of cells

Table 13: Overview of competition filter counts and extrapolation calculations of the constant light (CL) per replicate

Day	Rep.	Total cells ml^{-1}	SHTV-CAM-filter count cells ml^{-1}	SHTV-CAM-filter (%) count	SHTV-CAM-filter (%) upper limit	SHTV-CAM-filter (%) lower limit	SHTV-CAM-filter (%) filter spread	Extrapolated SHTV (%) SHTV-CAM-filter	Extrapolated Erk (%) SHTV-CAM-filter	Erk-CAM-filter count cells ml^{-1}	Erk-CAM-filter (%) count	Erk-CAM-filter (%) upper limit	Erk-CAM-filter (%) lower limit	Erk-CAM-filter (%) filter spread	Extrapolated Erk (%) Erk-CAM-filter	Extrapolated SHTV (%) Erk-CAM-filter	Mean extrapolated SHTV (%)	Mean extrapolated Erk (%)
7	1	4990	1850	37.0	44.4	18.0	26.5	72.0	28.0	4240	84.9	79.5	92.0	12.5	43.0	57.0	64.5	35.5
7	2	4651	1868	40.0	44.4	18.0	26.5	83.2	16.6	3994	85.9	79.5	92.0	12.5	50.8	49.1	66.3	33.7
7	3	4003	1345	33.3	44.4	18.0	26.5	57.8	42.2	3533	88.7	79.5	92.0	12.5	73.6	26.6	42.2	57.8
7	4	6375	2735	43.0	44.4	18.0	26.5	94.8	5.5	5255	82.8	79.5	92.0	12.5	26.0	73.9	84.2	15.8
7	5	2968	1350	45.6	44.4	18.0	26.5	97.6	2.2	2535	85.4	79.5	92.0	12.5	47.4	52.6	75.2	24.8
13	1	10677	5819	54.6	74.9	32.9	42.1	51.6	48.4	8597	80.4	64.0	91.7	27.7	59.2	40.8	46.2	53.8
13	2	14803	7098	47.8	74.9	32.9	42.1	35.6	64.6	12570	85.1	64.0	91.7	27.7	76.0	23.8	29.6	70.4
13	3	11190	5660	50.6	74.9	32.9	42.1	42.0	57.9	9683	86.5	64.0	91.7	27.7	81.0	18.5	30.3	69.7
13	4	13137	6450	48.8	74.9	32.9	42.1	37.8	62.0	11211	85.4	64.0	91.7	27.7	77.4	22.6	30.3	69.7
13	5	13991	6005	42.5	74.9	32.9	42.1	23.0	77.1	12426	89.0	64.0	91.7	27.7	90.8	9.4	16.2	83.8
16	2	19856	16618	83.7	86.9	58.5	28.4	89.0	11.3	16590	83.6	81.2	95.8	14.5	16.0	84.0	86.4	13.6
16	3	13675	11480	83.9	86.9	58.5	28.4	89.4	10.5	11421	83.6	81.2	95.8	14.5	16.2	84.0	86.8	13.2
16	4	17907	14759	82.5	86.9	58.5	28.4	84.4	15.7	15347	85.7	81.2	95.8	14.5	30.6	69.4	76.8	23.2
16	5	8259	7160	86.7	86.9	58.5	28.4	98.5	1.3	6496	78.7	81.2	95.8	14.5	1.8	98.2	98.4	1.6
20	1	32993	26113	79.1	88.8	41.6	47.1	79.4	20.5	24370	73.9	34.5	92.2	57.7	68.2	31.7	55.6	44.4
20	2	31274	23043	73.7	88.8	41.6	47.1	68.0	32.0	24693	78.9	34.5	92.2	57.7	77.0	23.0	45.5	54.5
20	3	32528	24830	76.4	88.8	41.6	47.1	73.8	26.3	24919	76.6	34.5	92.2	57.7	72.8	27.0	50.4	49.6
20	4	30175	23892	79.3	88.8	41.6	47.1	80.0	20.1	22656	75.1	34.5	92.2	57.7	70.4	29.6	54.7	45.3
20	5	30746	24910	81.1	88.8	41.6	47.1	83.8	16.3	22583	73.5	34.5	92.2	57.7	67.6	32.4	58.1	41.9
22	1	37885	32900	86.9	95.8	53.2	42.6	79.2	21.0	29627	78.3	46.0	93.0	47.0	69.0	31.3	55.1	44.9
22	2	46818	39044	83.4	95.8	53.2	42.6	71.0	29.1	37735	80.5	46.0	93.0	47.0	73.4	26.6	48.8	51.2
22	3	37168	32433	87.3	95.8	53.2	42.6	80.0	20.0	28465	76.5	46.0	93.0	47.0	64.8	35.2	57.6	42.4
22	4	37373	32484	86.9	95.8	53.2	42.6	79.0	20.9	28731	76.9	46.0	93.0	47.0	65.8	34.3	56.7	43.3
22	5	33887	29745	87.9	95.8	53.2	42.6	81.4	18.6	26441	77.9	46.0	93.0	47.0	67.8	32.2	56.8	43.2
26	1	49514	34339	69.5	92.6	39.1	53.6	56.6	43.2	45835	92.5	81.9	96.6	14.7	71.8	27.9	42.3	57.7
26	2	60843	43863	72.3	92.6	39.1	53.6	62.0	37.9	54680	89.7	81.9	96.6	14.7	53.2	46.7	54.4	45.6
26	3	40892	30474	74.5	92.6	39.1	53.6	66.4	33.8	36505	89.3	81.9	96.6	14.7	50.2	49.8	58.0	42.0
26	4	34778	25518	73.4	92.6	39.1	53.6	64.2	35.8	32033	92.2	81.9	96.6	14.7	69.8	30.0	47.1	52.9
26	5	40168	30283	75.3	92.6	39.1	53.6	68.0	32.3	36344	90.5	81.9	96.6	14.7	58.8	41.3	54.5	45.5

Table 14: Overview of competition filter counts and extrapolation calculations of the fluctuating light (FL) per replicate

Day	Rep.	Total cells ml^{-1}	SHTV-CAM-filter count cells ml^{-1}	SHTV-CAM-filter (%) count	SHTV-CAM-filter (%) upper limit	SHTV-CAM-filter (%) lower limit	SHTV-CAM-filter (%) filter spread	Extrapolated SHTV (%) SHTV-CAM-filter	Extrapolated Erk (%) SHTV-CAM-filter	Erk-CAM-filter count cells ml^{-1}	Erk-CAM-filter (%) count	Erk-CAM-filter (%) upper limit	Erk-CAM-filter (%) lower limit	Erk-CAM-filter (%) filter spread	Extrapolated Erk (%) Erk-CAM-filter	Extrapolated SHTV (%) Erk-CAM-filter	Mean extrapolated SHTV (%)	Mean extrapolated Erk (%)
7	1	3633	2200	60.2	80.0	38.2	41.8	52.4	47.3	2583	71.6	67.1	87.4	20.3	27.2	72.9	62.8	37.2
7	2	5139	2959	57.5	80.0	38.2	41.8	46.2	53.7	3756	74.3	67.1	87.4	20.3	35.6	64.3	55.3	44.7
7	3	4181	2712	64.9	80.0	38.2	41.8	63.8	36.3	2910	69.8	67.1	87.4	20.3	16.6	83.5	73.6	26.4
7	4	4213	2598	61.8	80.0	38.2	41.8	56.6	43.5	2933	69.7	67.1	87.4	20.3	12.6	87.5	72.0	28.0
7	5	4696	2854	60.8	80.0	38.2	41.8	54.2	45.9	3385	72.2	67.1	87.4	20.3	25.0	75.0	64.6	35.4
13	1	8123	5369	66.0	78.6	46.4	32.2	61.0	39.0	6935	85.6	80.6	94.0	13.5	37.4	62.4	61.7	38.3
13	2	9995	6650	66.9	78.6	46.4	32.2	63.6	36.5	8428	84.1	80.6	94.0	13.5	26.6	73.4	68.4	31.6
13	3	10975	7535	69.0	78.6	46.4	32.2	70.0	30.0	8885	80.9	80.6	94.0	13.5	3.6	96.4	83.2	16.8
13	4	11646	7576	65.0	78.6	46.4	32.2	57.8	42.2	9955	85.5	80.6	94.0	13.5	36.6	63.5	60.6	39.4
13	5	13432	7825	58.5	78.6	46.4	32.2	37.6	62.4	11777	87.2	80.6	94.0	13.5	49.4	50.5	44.1	55.9
16	1	10036	7019	70.0	79.6	43.5	36.2	73.4	26.6	8399	83.6	79.0	96.7	17.7	26.4	73.7	73.5	26.5
16	2	11079	7981	72.1	79.6	43.5	36.2	79.4	20.7	8925	80.6	79.0	96.7	17.7	10.6	89.4	84.3	15.7
16	3	13833	9924	72.3	79.6	43.5	36.2	79.8	20.3	11078	80.0	79.0	96.7	17.7	9.0	90.7	85.2	14.8
16	4	7622	5286	70.3	79.6	43.5	36.2	74.0	25.8	6260	81.8	79.0	96.7	17.7	16.0	83.9	79.1	20.9
16	5	12740	8658	68.1	79.6	43.5	36.2	68.0	32.0	10879	85.4	79.0	96.7	17.7	36.2	63.9	66.0	34.0
20	1	14840	10583	71.2	85.5	35.1	50.4	71.6	28.3	11796	79.5	57.3	94.4	37.1	59.8	40.1	55.9	44.1
20	2	13433	9620	71.7	85.5	35.1	50.4	72.6	27.3	10282	76.4	57.3	94.4	37.1	51.6	48.4	60.5	39.5
20	3	12928	9196	71.1	85.5	35.1	50.4	71.4	28.6	9999	77.3	57.3	94.4	37.1	54.2	46.0	58.7	41.3
20	4	17870	12434	69.5	85.5	35.1	50.4	68.2	31.7	13800	77.2	57.3	94.4	37.1	53.6	46.2	57.2	42.8
20	5	16095	11220	69.7	85.5	35.1	50.4	68.6	31.3	12577	78.2	57.3	94.4	37.1	56.0	43.7	56.2	43.8
22	1	20765	13419	64.8	76.0	31.3	44.7	74.8	25.0	17805	85.7	75.3	94.9	19.7	53.2	46.9	60.9	39.1
22	2	21373	14335	67.2	76.0	31.3	44.7	80.2	19.7	17812	83.2	75.3	94.9	19.7	40.4	59.5	69.9	30.1
22	3	20687	13759	66.7	76.0	31.3	44.7	79.2	20.9	17304	83.6	75.3	94.9	19.7	42.2	57.6	68.4	31.6
22	4	22266	14249	64.1	76.0	31.3	44.7	73.4	26.6	18588	83.5	75.3	94.9	19.7	41.8	57.9	65.6	34.4
22	5	18057	11514	64.0	76.0	31.3	44.7	73.0	26.9	15324	84.7	75.3	94.9	19.7	47.8	52.2	62.6	37.4
26	1	24548	19924	81.2	92.1	45.6	46.4	76.8	23.4	19628	79.9	72.0	95.7	23.7	33.2	66.7	71.7	28.3
26	2	26600	21844	82.3	92.1	45.6	46.4	79.2	21.0	20962	78.7	72.0	95.7	23.7	28.4	71.8	75.4	24.6
26	3	26030	20743	79.9	92.1	45.6	46.4	73.8	26.2	20892	80.1	72.0	95.7	23.7	34.2	65.9	69.9	30.1
26	4	33525	26834	79.9	92.1	45.6	46.4	74.0	26.2	26853	80.1	72.0	95.7	23.7	34.3	65.6	69.7	30.3
26	5	22324	18104	81.2	92.1	45.6	46.4	76.6	23.3	17431	78.0	72.0	95.7	23.7	25.4	74.6	75.7	24.3